Mechanism of the Hydrolysis of Halogen Nitrates in Small Water Clusters Studied by Electronic Structure Methods

Jonathan P. McNamara and Ian H. Hillier*

Department of Chemistry, University of Manchester, Manchester, M13 9PL, U.K.

Received: January 4, 2001; In Final Form: May 18, 2001

High-level electronic structure calculations have been used to study the mechanism of the hydrolysis of bromine nitrate in neutral water clusters containing one to eight solvating water molecules. The calculations clarify some of the uncertainties in the mechanism of halogen nitrate hydrolysis on PSC ice aerosols. The free energy barrier decreases from 42.4 kcal mol^{-1} (single water) to essentially zero when catalyzed by six water molecules. As the size of the water cluster is increased, $BrONO_2$ shows increasing ionization along the $Br-ONO_2$ bond, consistent with the proposed predissociation in which the electrophilicity of the bromine atom is enhanced, thus making it more susceptible to nucleophilic attack from a surface water molecule. A species akin to the experimentally proposed intermediate, $H_2OBr^+NO_3^-$, is found to be stable in clusters containing both three and six water molecules, where the ion pair is separated by single and double layers of water molecules, respectively. For a cluster containing six water molecules, which has a structure related to that of ordinary hexagonal ice, $BrONO_2$ is hydrolyzed to yield HOBr and ionized nitric acid ($H_3O^+NO_3^-$). The calculations thus predict an ionic mechanism for the hydrolysis of halogen nitrates on PSC ice aerosols.

1. Introduction

Polar stratospheric cloud (PSC) ice aerosols have been recognized as the sites for the heterogeneous catalysis of a number of atmospherically important reactions which lead to the stratospheric depletion of ozone over Antarctica.[1−8] During the Antarctic winter, surface-catalyzed reactions convert halogen-containing compounds such as chlorine ($ClONO_2$) and bromine nitrate ($BrONO_2$) into the photochemically labile species HOCl and HOBr [reactions 1 and 2]

$$BrONO_{2(ads)} + H_2O_{(ads)} \rightarrow HOBr_{(ads)} + HONO_{2(ads)} \quad (1)$$

$$ClONO_{2(ads)} + H_2O_{(ads)} \rightarrow HOCl_{(ads)} + HONO_{2(ads)} \quad (2)$$

These species are then photolyzed in the spring to yield Cl/ClO[9−11] and Br/BrO[9−18] radicals responsible for the "sudden" ozone loss phenomenon.

Wofsy et al.[12] were the first to implicate bromine radicals as catalysts for the destruction of ozone. More recently, in-situ measurements have shown that halogen radical chemistry accounts for up to one-third of the photochemical removal of ozone, where reactions involving BrO account for one-half of this loss.[9] While the total atmospheric abundance of organic chlorine has peaked at 3700 parts per trillion volume (pptv),[19] the total bromine loading in the lower stratosphere is increasing,[19] with estimates in the range of 10−20 pptv.[12,13,19] Despite its lower abundance, bromine reactions are important due to the relatively short photolytic lifetime of the reservoir species $BrONO_2$ and HOBr. Bromine nitrate itself has a photolysis rate of 1000 s^{-1}, suggested to be up to 20 times more rapid than that of $ClONO_2$.[20−22] Thus, bromine radicals can initiate catalytic cycles leading to the conversion of H_2O into HO_x, HCl into ClO, and NO_x into $HONO_2$, leading to ozone loss at all latitudes and for all seasons, most notably in a sulfate-perturbed atmosphere.[18,23] In an atmospheric simulation, studying the role of aerosols in ozone depletion, Solomon et al.[3] attribute discrepancies between calculated and observed ozone losses to the hydrolysis of $BrONO_2$ [reaction 1], and calculations by Tie and Brasseur[13] suggest the heterogeneous catalysis of reactions 1 and 3 on sulfate aerosols could lead to ozone losses of 2−3% under post-volcanic conditions

$$HOBr_{(ads)} + HCl_{(ads)} \rightarrow BrCl_{(ads)} + H_2O_{(ads)} \quad (3)$$

Despite the potential stratospheric impact of $BrONO_2$ hydrolysis, there have only been a limited number of experimental studies. Hanson and Ravishankara[24] have used kinetics techniques to obtain uptake (sticking) coefficients, γ, for $BrONO_2$ of 0.4 on 60 wt % H_2SO_4 solutions, almost 2 orders of magnitude greater than that for $ClONO_2$ ($\gamma \approx 0.003$).[24] Sticking coefficients for $BrONO_2$ have also been measured on water-ice, with and without added HCl.[25,26] Such experiments have also shown the hydrolysis of $ClONO_2$ [reaction 2] to be efficient at stratospheric conditions (ca. 180 K) on NAT (nitric acid trihydrate, type I PSC),[27,28] water-ice (type II PSC),[28,29] and sulfate aerosols,[30−34] which are found throughout the atmosphere. A recent reflection−absorption infrared spectroscopy (RAIRS) study by Gane and Sodeau[35] suggests that the hydrolysis of $BrONO_2$ may be mechanistically close to that of $ClONO_2$.[36−40] They report evidence for two competing mechanisms operating on ice-films at 95−185 K. At 185 K, an ionic mechanism is proposed involving the hypobromous ion (H_2OBr^+) intermediate leading to reaction products involving nitric acid dihydrate (NAD) or NAT. In contrast, at lower temperatures and limited water availability, a molecular mechanism is proposed leading to products involving hydrated nitric acid.

On the mechanistic side, the idea that the heterogeneous hydrolysis of $ClONO_2$ [reaction 2] can be effected by a small number of water molecules is now well established.[41−50] Both

* Corresponding author. Fax: 0161 275 4734. E-mail: Ian.Hillier@man.ac.uk.

10.1021/jp0100304 CCC: $20.00
Published on Web 06/29/2001

TABLE 1: Structural Parameters of $BrONO_2$

parameter[a]	B3LYP/6-311++G(d,p)	MP2/6-311++G(d,p)	CCSD(T)/TZ2P[b]	experiment[c]
$r(Br_1-O_2)$	1.865	1.854	1.848	1.829
$r(O_2-N_3)$	1.483	1.524	1.490	1.456
$r(N_3-O_4)$	1.193	1.196	1.199	1.205
$r(N_3-O_5)$	1.192	1.193	1.198	1.205
$\angle(Br_1O_2N_3)$	115.5	113.4	113.5	113.9
$\angle(O_2N_3O_4)$	109.1	108.1	109.2	106.6
$\angle(O_2N_3O_5)$	118.2	117.6	118.2	119.5

[a] Bond lengths in Å and angles in deg; $BrONO_2$ is planar. Refer to Figure 1a for atom labeling. [b] Parthiban and Lee.[51] [c] Electron diffraction data.[82]

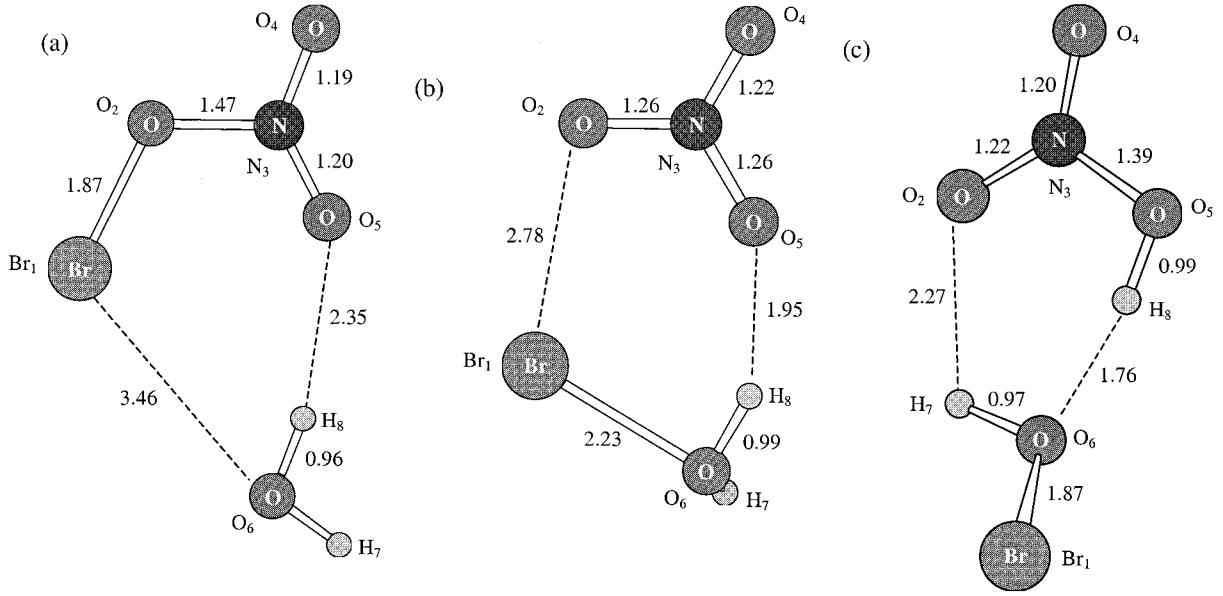

Figure 1. Stationary structures for $BrONO_2 + (H_2O)$ reaction: (a) reactants, (b) transition state, and (c) products ($HOBr/HONO_2$). In this and subsequent figures, all distances are in Å and correspond to the optimized B3LYP/6-311++G(d,p) geometries unless otherwise stated.

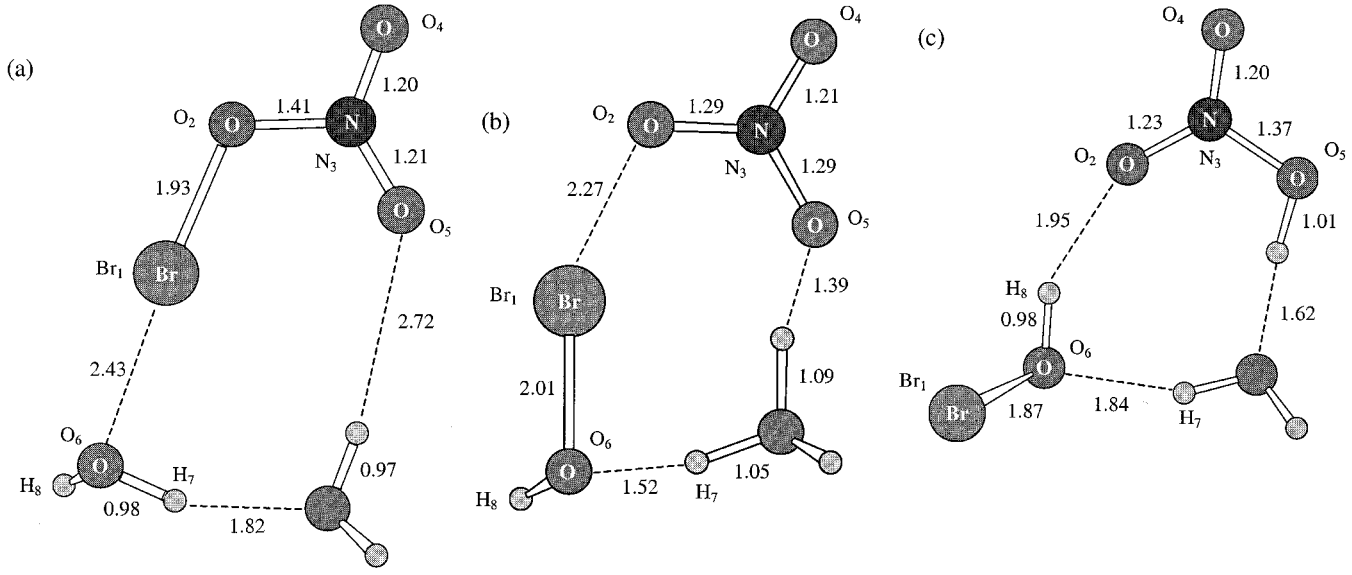

Figure 2. Stationary structures for $BrONO_2 + (H_2O)_2$ reaction: (a) reactants, (b) transition state, and (c) products [$HOBr/HONO_2 \cdot (H_2O)$].

the single-water and PSC-catalyzed hydrolysis reactions have been studied using electronic structure methods. Akhmatskaya et al.[44] have calculated a barrier of 44.7 kcal mol^{-1} for hydrolysis involving a single water, whereas Bianco and Hynes[45] have identified the ionic products (HOCl and $H_3O^+NO_3^-$) along an MP2//HF/6-31G+(d,p) microsolvated reaction path, where the barrier is ca. 3 kcal mol^{-1}. Calculations using large basis sets and density functional theory (DFT) of the hydrolysis of $ClONO_2$ in a six-water cluster related to hexagonal ice also predict a facile reaction.[41,42] As for $BrONO_2$, theoretical studies have mainly focused on the structure of $BrONO_2$ itself. Parthiban and Lee[51] have calculated the structure and heat of formation of $BrONO_2$ at the CCSD(T)/TZ2P level, and Ying and Zhao[52] have used both ab initio and DFT methods to study the interaction of HOBr and $BrONO_2$ with single water molecules. The structures and harmonic frequencies of a range of atmospheric bromine compounds ($XONO_2$, X = Br, OBr, and O_2-Br) have also been calculated at the B3LYP/TZ2P level.[53]

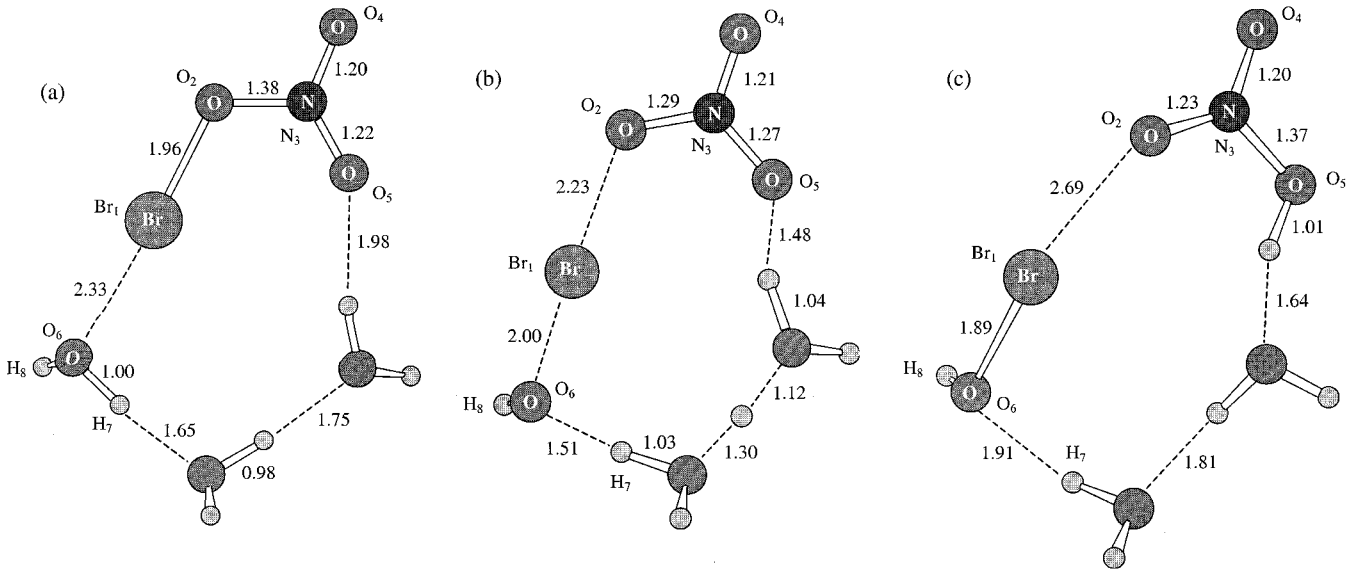

Figure 3. Stationary structures for $BrONO_2 + (H_2O)_3$ reaction: (a) reactants, (b) transition state, and (c) products [$HOBr/HONO_2 \cdot (H_2O)_2$].

However, to date there have been no theoretical studies regarding the hydrolysis of $BrONO_2$.

In this paper, we present the results of both ab initio (MP2) and DFT calculations designed to understand the reactivity of $BrONO_2$ in small water clusters. The calculations further clarify the mechanism of halogen nitrate hydrolysis on PSC ice aerosols. The catalytic role of water in effecting the predissociation of $BrONO_2$ is examined, whereby ionization along the $Br-ONO_2$ bond serves to increase the electrophilicity of the bromine atom, an effect well documented for $ClONO_2$.[39−42] Laboratory studies of the hydrolysis of $BrONO_2$ and Br_2 report mechanisms involving a hypobromous ion intermediate (H_2OBr^+).[35,54] Our calculations explore possible mechanisms of formation of the hypobromous ion and compare this species with the related hypochlorous ion (H_2OCl^+) implicated in the hydrolysis of $ClONO_2$.[36−42] RAIRS experiments[35] suggest that two competing hydrolysis pathways are accessible under stratospheric conditions, the ionic mechanism being favored when excess water is available at the PSC ice aerosol surface

$$BrONO_{2(ads)} + H_2O_{(ads)} \rightarrow H_2OBr^+_{(ads)} + NO_3^-{}_{(ads)} \quad (4a)$$

$$H_2OBr^+_{(ads)} + NO_3^-{}_{(ads)} \rightarrow HOBr_{(ads)} + HONO_{2(ads)} \quad (4b)$$

To investigate both the ionic [reaction 4] and molecular [reaction 1] reaction pathways, we have studied the hydrolysis reaction in water clusters containing one to eight solvating waters in order to account for different solvating environments at the ice surface. To understand how $BrONO_2$ interacts with the ice surface at a molecular level, we have calculated harmonic frequencies for our clusters containing $BrONO_2$ or $H_2OBr^+NO_3^-$ in order to help interpret the available IR data.[35] In light of our calculations, the implications for atmospheric halogen chemistry are discussed.

2. Modeling PSC Ice Aerosols

The role of PSC ice aerosols in low temperature heterogeneous catalysis is currently of great interest. However, to date the construction and orientation of water molecules at the PSC surface remain unclear. Materer et al.[56] have probed the surface of an ice film crystallized on a Pt(111) surface at 90 K. Using LEED and combined ab initio and molecular dynamics (MD) calculations, they suggest that the ice surface has full bilayer termination. FTIR spectroscopy and MD/Monte Carlo simulations have been used to probe the interaction of adsorbates with ice-like surfaces.[57−61] Importantly, these investigations reveal the presence of rings of water molecules on the ice surface that are large enough to accommodate several adsorbate species and that are also proposed as the sites for acid ionization.[61]

Electronic structure methods have been successful in studying the interaction of small atmospherically relevant species such as HOCl and HCl with the ice surface. Geiger et al.[62] have used a four-water cluster excised from the ideal surface of hexagonal ice, and Robinson Brown and Doren[63] have studied the interaction of HOCl with both $(H_2O)_4$ and $(H_2O)_{26}$ cluster models excised from the ideal hexagonal ice crystal. In contrast, a number of atmospheric reactions have been studied in small water clusters. The mechanism of the oxidation of SO_2 by H_2O_2 in water droplets has been elucidated by Vincent et al.,[64] and Smith et al.[65] have investigated the process of acid dissociation. Such clusters have been used to study the hydrolysis of SO_3,[44,66] $ClONO_2$,[41−50] and N_2O_5[67−69] and the reactions of $ClONO_2$[70−73] and N_2O_5 with HCl,[74] and they allow for ionization and solvation of key intermediates and products, an effect absent in models based on the ideal ice surface.[62,63] In view of Buch's findings[61] and the proposed dynamic nature of the ice surface,[75] we have chosen to study the hydrolysis of bromine nitrate in water clusters relevant to the study of reactions on both the PSC aerosol surface and in small water droplets.

3. Computational Method

The electronic structure calculations reported herein have been carried out using the GAUSSIAN 94[76] and GAUSSIAN 98[77] suites of programs. Electron correlation has been included using density functional theory (B3LYP)[78−80] and Møller Plesset perturbation theory (MP2).[81] For the larger systems studied, DFT was chosen in order to minimize computational expense, MP2 optimizations being too time-consuming for systems having ca. 400 basis functions. The B3LYP functional was chosen following a recent study[51] in which the structure of isolated $BrONO_2$ calculated at this level (Table 1) is in excellent agreement with MP2, CCSD(T), and electron diffraction data.[82] Recent electronic structure calculations[41−43,67,73,74] have highlighted the need for both polarization and diffuse functions in order to accurately describe hydrogen-bonded systems. For this reason, the flexible 6-311++G(d,p) basis set was used for all

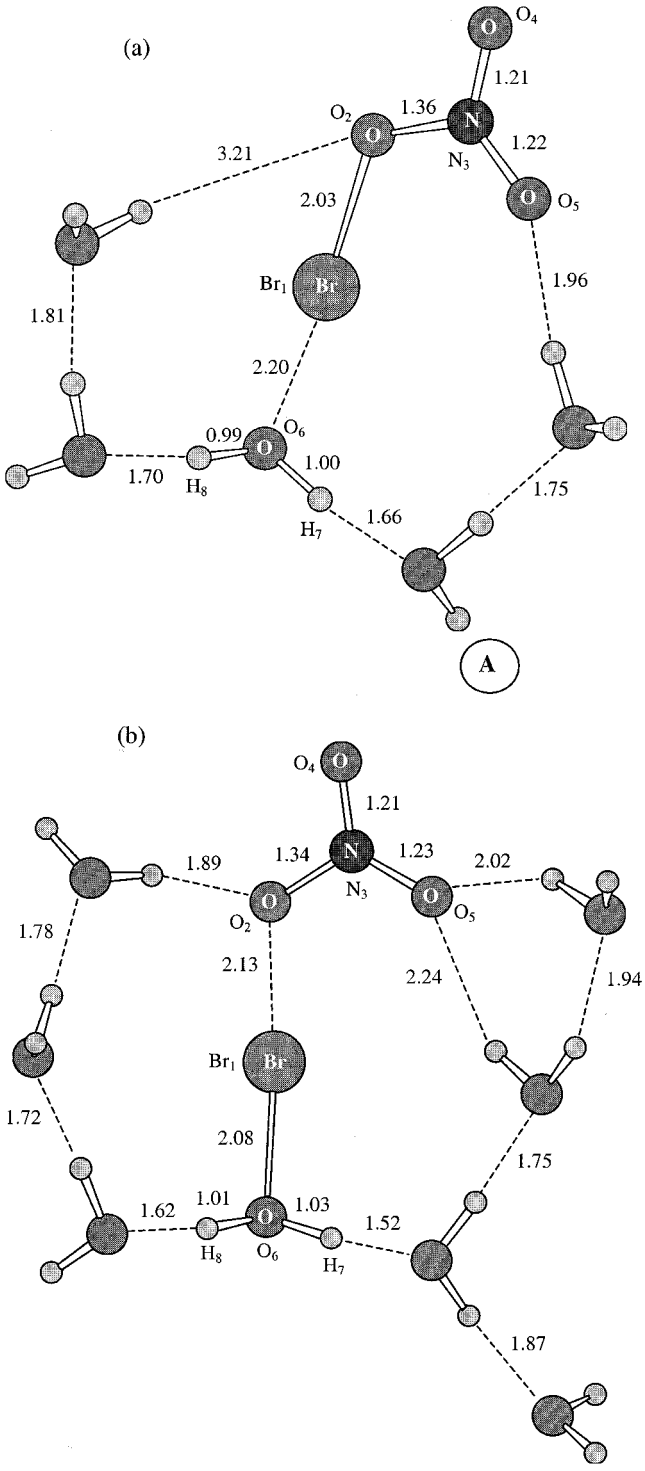

Figure 4. (a) Reactant structure $BrONO_2 \cdot (H_2O)_5$ showing bromine nitrate solvated by five water molecules. (b) Ion pair structure $BrONO_2 \cdot (H_2O)_8$ showing bromine nitrate solvated by eight water molecules.

DFT optimizations. For comparison, single-point energy calculations have been carried out at the MP2/6-311++G(3df,-3pd)//B3LYP/6-311++G(d,p) level. Stationary structures were characterized as minima or transition structures on the potential energy surface by calculation of harmonic vibrational frequencies. Intrinsic reaction coordinate (IRC) calculations were performed to confirm that each transition state (TS) did indeed connect the reactant and product minima. Because of the size of the systems studied (ca. 400 basis functions), the IRC calculations were restricted to the region close to the TS, the final point in each direction being optimized to obtain the

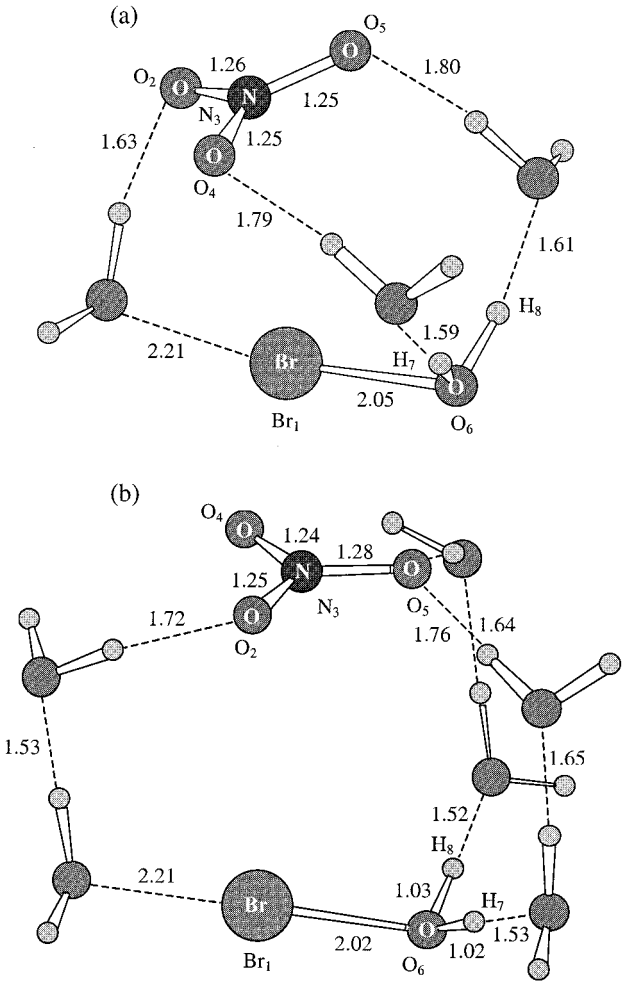

Figure 5. (a) Ion pair structure $H_2OBr^+ \cdot (H_2O)_3 \cdot NO_3^-$ showing solvated hypobromous and nitrate ions. (b) Ion pair structure $H_2OBr^+ \cdot (H_2O)_6 \cdot NO_3^-$ showing solvated hypobromous and nitrate ions.

reactant and product complexes. Free energies were calculated within the perfect gas, rigid rotor, harmonic oscillator approximation at 180 K, a temperature appropriate to that of the stratosphere.

4. Computational Results

In discussing the various structures, we refer to the atom numbering scheme of the reactant pair (Figure 1a), containing $BrONO_2$ and the attacking nucleophile, H_2O. We have considered essentially two different types of cluster models. The first, ring structures (Figures 1−4) contain $BrONO_2$ solvated by single rings of water molecules. The second, ice-like structures, contain either the ion pair $H_2OX^+NO_3^-$ (X = Cl or Br, Figures 5 and 6) or $BrONO_2$ (Figure 7) solvated by single and double layers of water molecules. The structures are denoted by the number of complete waters they contain before reaction and, a reactant structure is defined as a system in which bromine has not transferred to the attacking nucleophile, H_2O. Individual structural parameters are at the B3LYP/6-311++G(d,p) level unless otherwise stated. Energies of all structures are given in Table 2. The energies of binding (Table 2) are defined as the difference between the energy of the optimized cluster containing $BrONO_2$ and the sum of the energies for the isolated $BrONO_2$ and water cluster fragments. The energy barriers are given in Table 3. The minimum-energy pathways (MEP) for hydrolysis in one-, two-, and three-water clusters derived from the IRC calculations are shown in Figures 8−10 for a thorough analysis of the reaction mechanisms.

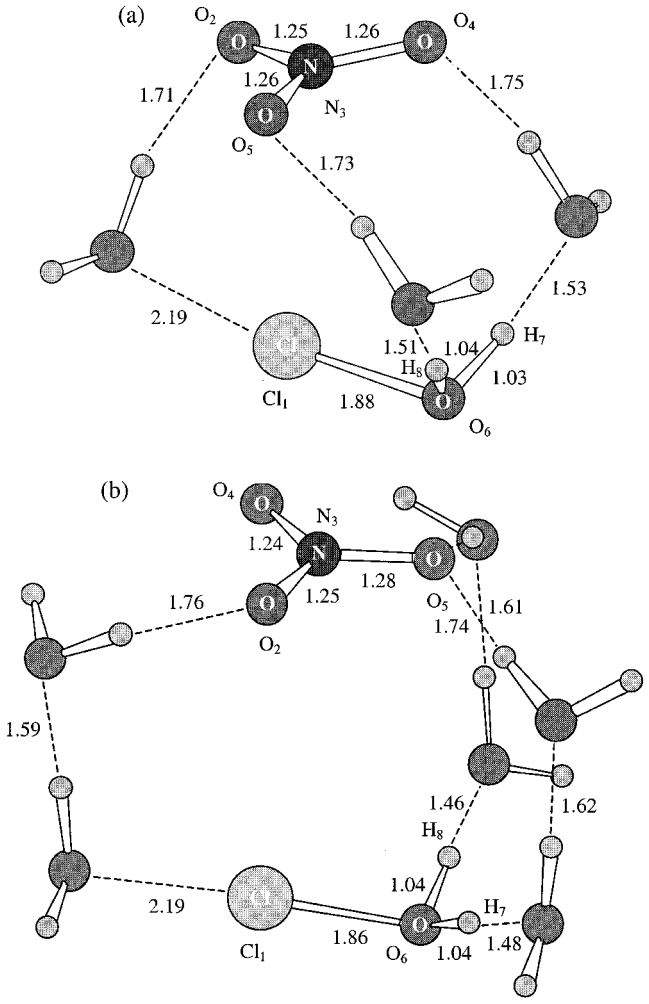

Figure 6. (a) Ion pair structure $H_2OCl^+ \cdot (H_2O)_3 \cdot NO_3^-$ showing solvated hypochlorous and nitrate ions. (b) Ion pair structure $H_2OCl^+ \cdot (H_2O)_6 \cdot NO_3^-$ showing solvated hypochlorous and nitrate ions.

A. Gas-Phase $BrONO_2$. We first discuss the structure of free $BrONO_2$. The B3LYP/6-311++G(d,p) structure and the MP2, CCSD(T), and electron diffraction structures[82] are given in Table 1 for comparison. The DFT geometry is in excellent agreement with both the MP2[83] and the CCSD(T) structures.[51,53] Comparison with electron diffraction data reveals that the largest discrepancy between calculation (B3LYP) and experiment occurs in the Br_1-O_2 and O_2-N_3 bonds (1.865 and 1.483 Å) being a little longer than those in the experiment (1.829 and 1.456 Å). However, the B3LYP structure represents a considerable improvement over the structure at the HF level,[84] where an O_2-N_3 distance of 1.36 Å overestimates the ionicity of this species. Having briefly considered the structure of free $BrONO_2$, we now consider the structural effects of solvation in one to eight water molecules.

B. Structure and Reactivity of $BrONO_2$. *Ring Structures.* We now consider a range of clusters in which $BrONO_2$ is solvated by one to eight water molecules, where the arrangement of the water molecules may be related to the rings of waters reported on the ice surface by Buch et al.[61] These rings are suggested to be large enough to accommodate several adsorbate species and are also proposed as the sites for acid ionization. As a consequence of the proposed dynamic nature of the ice surface,[75] it is likely that adsorbate molecules will be further solvated by surface-bound waters. Thus, our ring structures (Figures 1−4) highlight the role of water in catalyzing halogen nitrate reactions. First, the addition of water molecules leads to both a lengthening of the Br_1-O_2 and shortening of the O_2-N_3 bonds, consistent with $BrONO_2$ ionizing toward $Br^{\delta+}NO_3^{\delta-}$, analogous to $ClONO_2$ ionization.[39−42] Mulliken charges (Table 4) further support the idea that additional waters enhance ionization, leading to notable charge transfer from the nucleophile (H_2O). Frontier molecular orbital theory reveals efficient overlap between the HOMO of H_2O and the LUMO of $ClONO_2$,[38] facilitating charge transfer, which is also the case for $BrONO_2$. The increased ionic interaction between $BrONO_2$ and the water cluster is reflected in a parallel increase in the binding energy of this species (Table 2). Thus, the ring structures may provide evidence for the proposed predissociation of $BrONO_2$, where ionization along the $Br-ONO_2$ bond serves to increase the electrophilicity of the bromine atom, which is thus prone to nucleophilic attack from H_2O.[39−42]

Our initial model system contains $BrONO_2$ solvated by a single water molecule (Figure 1a). This minimum has previously been identified by Ying and Zhao[52] and is closely related to structures where $ClONO_2$ is hydrolyzed with barriers of 44.7 [B3LYP/6-311+G(d,p)][44] and 68.1 kcal mol^{-1} [MP2//HF/6-31G(d)].[47] For this one-water structure, $BrONO_2$ is hydrolyzed with a barrier of 42.4 kcal mol^{-1} (72.7 kcal mol^{-1}, MP2), a little lower than that for the single-water hydrolysis of $ClONO_2$ at this level (48.8 kcal mol^{-1}, Table 3).[43,74] The MEP (Figure 8) involves an S_N2 attack of O_6 (of H_2O) at Br_1, leading to the transfer of Br_1 to the nucleophile. The transition state (TS, imaginary frequency 151 cm^{-1}, Figure 1b) contains species akin to protonated hypobromous acid (H_2OBr^+) and nitrate (NO_3^-) and resembles the six-membered cyclic TS proposed by Hanson[85] for hydrolysis of $ClONO_2$. Notable charge separation in the TS is supported by charges of 0.45 and −0.45 on the H_2OBr and NO_3 entities, respectively (Table 4). Collapse of the TS, via proton transfer to the developing nitrate leads to the reaction products involving the molecular acids ($HONO_2$ and HOBr, Figure 1c).

The formation of species akin to the $H_2OBr^+NO_3^-$ ion pair in the one-water TS suggests the addition of an extra ring water may stabilize charge separation. Thus, we have examined the structural and energetic effects of the addition of an extra ring water. The barrier for $BrONO_2$ hydrolysis involving two-water molecules is 22.1 kcal mol^{-1} (24.0 kcal mol^{-1}, MP2, Table 3), a decrease of 20.3 kcal mol^{-1} compared to that for the one-water reaction and close to that for $ClONO_2$ hydrolysis (22.4 kcal mol^{-1}, Table 3).[43] In the reactant structure (Figure 2a), the Br_1-O_2 bond length is a little longer (1.93 Å) than that in the free molecule (1.87 Å, B3LYP), and there is some charge transfer to $BrONO_2$, which now has a charge of −0.13 (Table 4). The increased ionization of $BrONO_2$ within this structure is reflected in an increased binding energy of 13.8 kcal mol^{-1} compared to that for the one-water structure (2.1 kcal mol^{-1}). The MEP (Figure 9) highlights some important differences between the one- and two-water catalyzed reactions. The distinguishing feature of the two-water TS (Figure 2b) is that it involves a species close to H_3O^+, differing from the one-water TS (Figure 1b), which involves a species close to H_2OBr^+. Evidence supporting charge separation in the two-water TS is afforded by charges of 0.70 (H_3O) and −0.56 (NO_3), and the formation of HOBr is also well advanced with a Br_1-O_6 length of 2.01 Å (1.87 Å, free molecule, B3LYP). The path to products is characterised by proton transfer from the H_3O entity to O_5 of the forming nitrate to yield solvated $HONO_2$ and HOBr (Figure 2c). This structure is found to be only 2.0 kcal mol^{-1} more stable than reactants, whereas the reaction energy for the hydrolysis of $ClONO_2$ by two waters is −4.9 kcal mol^{-1} (Table

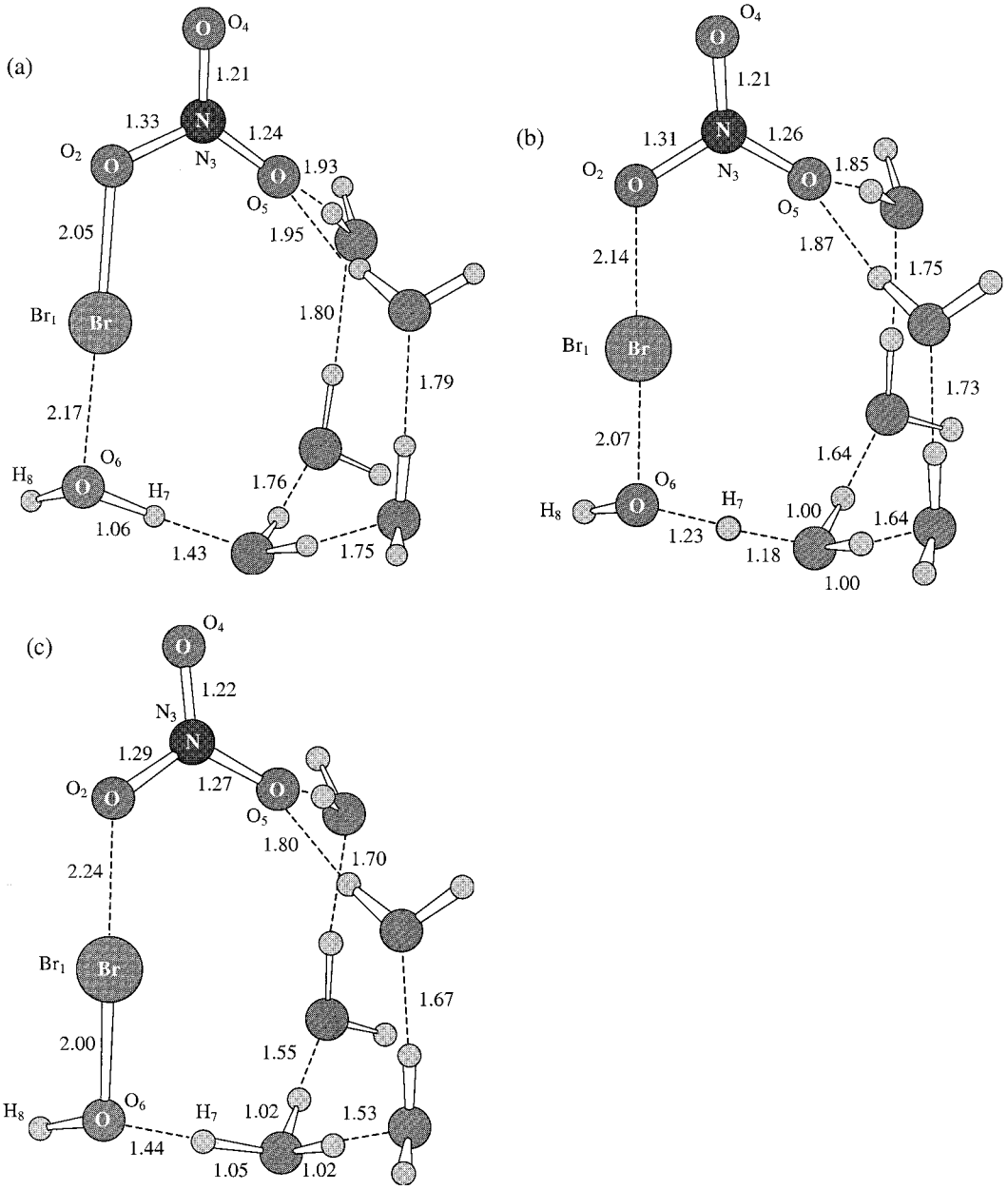

Figure 7. Stationary structures for $BrONO_2 + (H_2O)_6$ reaction: (a) reactants, (b) transition state, and (c) products $[H_3O^+ \cdot (H_2O)_4 \cdot NO_3^-/HOBr]$.

3). In the one- and two-water reactions discussed so far, the TSs contain species akin to $H_2OBr^+NO_3^-$ (one-water) and $H_3O^+NO_3^-$ (two-water). Since the addition of an extra water has clearly resulted in large structural changes in the TS, we have examined the effect of the addition of a further ring−water molecule.

To our two-water reactant cluster (Figure 2a), we have added an extra ring water molecule to form a three-water structure related to a fragment excised from the ideal ice surface.[45] The inclusion of the extra ring water results in a lowering of the free energy barrier to just 13.4 kcal mol^{-1} (14.4 kcal mol^{-1}, MP2) comparable to that for hydrolysis of $ClONO_2$ (14.5 kcal mol^{-1}, Table 3).[43] These barriers are somewhat lower than those calculated by Bianco and Hynes[45] [ca. 29 kcal mol^{-1}, HF/6-31+G(d,p)] and Xu and Zhao[47] [18.6 kcal mol^{-1}, MP2//HF/6-31G(d)] for the hydrolysis of $ClONO_2$ in a related three-water cluster. Notably, the reaction energy is 4.9 kcal mol^{-1}, which presumably would decrease upon further solvation. The MEP (Figure 10) follows closely that of the two-water assisted reaction in that the initial stages of the reaction involve nucleophilic attack of water (O_6 at Br_1), coupled with a proton transfer to an adjacent water. The TS (imaginary frequency 218 cm^{-1}, Figure 3b) is characterized by Br_1-O_2 and Br_1-O_6 bond breaking and forming distances of 2.23 and 2.00 Å, respectively. Structurally, the TS is close to that in the two-water catalyzed reaction (Figure 2b) containing species close to H_3O^+ and NO_3^-, forming a contact ion pair (CIP). There is notable charge separation within the TS, with charges of 0.69 (H_3O) and −0.61 (NO_3). Release of a proton to the developing nitrate yields the solvated molecular acids, $HONO_2$ and HOBr (Figure 3c).

Xu and Zhao[47] suggest additional waters may not only provide a bridge for the reaction coordinate (proton shuttle) but also enhance the ionic character of the reaction pathway through hydration. Hence, we have studied the further solvation of the three-water reactant cluster (Figure 3a). The addition of two bridging waters leads to a five-water cluster (Figure 4a) somewhat more polarized than the structures described so far. An increased intramolecular Br_1-O_2 distance of 2.03 Å (1.96 Å, three-water structure) and charges of −0.31 ($BrONO_2$) and 0.24 (H_2O) support the idea that $BrONO_2$ readily ionizes when

TABLE 2: Internal Energies (Hartrees) and Binding Energies (kcal mol^{-1}) of $BrONO_2$ Hydrolysis Structures

structure[a]		B3LYP/6-311++G(d,p)	MP2/6-311++G(3df,3pd)[b]	binding of $BrONO_2$[c]
		Ring Clusters		
$BrONO_2\cdot(H_2O)$[d]	R	−2930.925887	−2928.706982	2.1
	TS	−2930.861890	−2928.594693	
	P	−2930.935704	−2928.712588	
$BrONO_2\cdot(H_2O)_2$[e]	R	−3007.408975	−3005.050345	13.8
	TS	−3007.373782	−3005.012000	
	P	−3007.412203	−3005.054380	
$BrONO_2\cdot(H_2O)_3$[f]	R	−3083.888370	−3081.392883	22.0
	TS	−3083.865566	−3081.368459	
	P	−3083.879871	−3081.388679	
$BrONO_2\cdot(H_2O)_5$[g]		−3236.834616	−3234.069273	35.4
$BrONO_2\cdot(H_2O)_6$[h]		−3313.303477	−3310.403348	38.6
$BrONO_2\cdot(H_2O)_8$[i]		−3466.255062	−3463.086455	
		Cage Clusters		
$H_2OBr^+\cdot(H_2O)_3\cdot NO_3^-$[j]		−3160.346311	−3157.718955	
$H_2OBr^+\cdot(H_2O)_6\cdot NO_3^-$[k]		−3389.785966	−3386.750769	
$BrONO_2\cdot(H_2O)_6$[l]	R	−3313.308016	−3310.406730	43.3
	TS	−3313.307033	−3310.405372	
	P	−3313.307601	−3310.406555	

[a] R (reactants), TS (transition state), and P (products). [b] Single-point energy evaluations using B3LYP/6-311++G(d,p) structures. [c] B3LYP/6-311++G(d,p) level. [d] Figure 1. [e] Figure 2. [f] Figure 3. [g] Figure 4a. [h] Figure 4a solvated at A. [i] Figure 4b. [j] Figure 5a. [k] Figure 5b. [l] Figure 7.

TABLE 3: Reaction Energies and Barriers (kcal mol^{-1}) and Imaginary Frequencies of Transition States (cm^{-1})

		internal energy (0 K)				free energy (180 K)			
	imaginary	B3LYP/6-311++G(d,p)		MP2/6-311++G(3df,3pd)[a]		B3LYP/6-311++G(d,p)		MP2/6-311++G(3df,3pd)[b]	
structure	frequency	barrier	reaction	barrier	reaction	barrier	reaction	barrier	reaction
				Bromine Nitrate					
$BrONO_2\cdot(H_2O)$[c]	151	40.2	−6.2	70.5	−3.5	42.4	−3.0	72.7	−0.4
$BrONO_2\cdot(H_2O)_2$[d]	291	22.1	−2.0	24.1	−2.5	22.1	−2.0	24.0	−2.6
$BrONO_2.(H_2O)_3$[e]	218	14.3	5.3	15.3	2.6	13.4	4.9	14.4	2.2
$BrONO_2.(H_2O)_6$[f]	259	0.6	0.3	0.9	0.1	0.0	1.4	0.2	1.3
				Chlorine Nitrate					
$ClONO_2\cdot(H_2O)$[g]	175	47.7	−2.6	78.4	−1.3	48.8	−0.5	79.5	0.8
$ClONO_2\cdot(H_2O)_2$[h]	343	21.9	−5.0	25.7	−4.3	22.4	−4.9	26.2	−4.2
$ClONO_2\cdot(H_2O)_3$[h]	430	14.9	1.4	18.1	−0.6	14.5	1.1	17.7	−0.9
$ClONO_2\cdot(H_2O)_6$[i]	322	0.8	−1.3	1.9	−2.1	0.1	0.0	1.1	0.8

[a] Calculated using the B3LYP/6-311++G(d,p) structure. [b] Includes thermodynamic correction at the B3LYP/6-311++G(d,p) level. [c] Figure 1. [d] Figure 2. [e] Figure 3. [f] Figure 7. [g] McNamara and Hillier.[43,74] [h] McNamara and Hillier.[43] [i] McNamara and Hillier.[41−43]

the incipient nitrate is more fully solvated. Furthermore, the binding energy of $BrONO_2$ (35.4 kcal mol^{-1}) to the water cluster has increased by 13.4 kcal mol^{-1} compared to that of the three-water system (Figure 3a). Moreover, solvation at A of the five-water structure (Figure 4a) by a single water (not shown) leads to a further increase in the binding energy (of $BrONO_2$) by 3.2−38.6 kcal mol^{-1} (Table 2). We conclude that waters in the second solvation shell may not actively participate in the reaction but can assist binding $BrONO_2$ to the ice aerosol surface so that reaction can take place.

In a study of the hydrolysis of $ClONO_2$, McNamara and Hillier[42] identify a structure in which $ClONO_2$ is solvated by eight water molecules such that the transferring chlorine is closer to the attacking nucleophile (H_2O) than to the departing nitrate, thus forming a $H_2OCl^+NO_3^-$ contact ion pair (CIP) (see Figure 8 of ref 42).[36−42] We have identified an analogous structure in which $BrONO_2$ is solvated by eight water molecules and is related to the five-water cluster (Figure 4a) but has additional solvating water inserted into each ring (Figure 4b). Compared to our previous structures this one shows a further lengthening and shortening of the Br−O intra- and intermolecular distances (2.13 and 2.08 Å), but the formation of a well-defined hypobromous acid molecule is not seen. The H_2OBr (Br−O, 2.08 Å) entity has a structure that differs somewhat from the isolated molecule (Br−O, 1.93 Å, B3LYP), with also some lengthening of the O−H bonds to 1.01 and 1.03 Å. Further evidence that the reaction is far from complete is afforded by formal charges of 0.50 and −0.59 on the H_2OBr and NO_3 entities (Table 4). A recent RAIRS study by Gane and Sodeau[35] suggests the H_2OBr^+ entity to be an intermediate in $BrONO_2$ hydrolysis. The formation of a CIP in our eight-water structure may explain the spectral features attributed to a nitrate ion asymmetrically solvated.[35] McNamara and Hillier[42] also calculate an eight-water cluster containing both HOCl and the $H_3O^+NO_3^-$ CIP, in which the ions are separated by a relatively short hydrogen bond of 1.66 Å (see Figure 9 of ref 42). This second ion pair structure was found to be only 1.5 kcal mol^{-1} more stable than the structure involving H_2OCl^+. However, we were unable to locate an analogous structure containing both HOBr and the $H_3O^+NO_3^-$ CIP.

Ice-Like Structures. Turning now to consider a second type of cluster model, ice-like structures, Smith et al.[65] report ab initio calculations of acid dissociation in small water clusters, where the ion pair $H_3O^+\cdot(H_2O)_n\cdot X^-$ (X = F, Cl, SH, HSO_3 and HSO_4) has been shown to form stable zwitterionic structures when separated by single and double layers of water molecules (n = 3 or 6). In line with this, calculations of the hydrolysis of Br_2 by Ramondo et al.[54] have shown both the $H_2OBr^+\cdot(H_2O)_n\cdot Br^-$ and $H_3O^+\cdot(H_2O)_n\cdot BrOH^-$ ion pairs to be stable with 3 or 6 water molecules. McNamara and Hillier[41,42] have also shown that the hydrolysis of $ClONO_2$ in a six-water cluster structurally related to hexagonal ice leads to the ionic products $H_3O^+\cdot(H_2O)_4\cdot NO_3^-$/

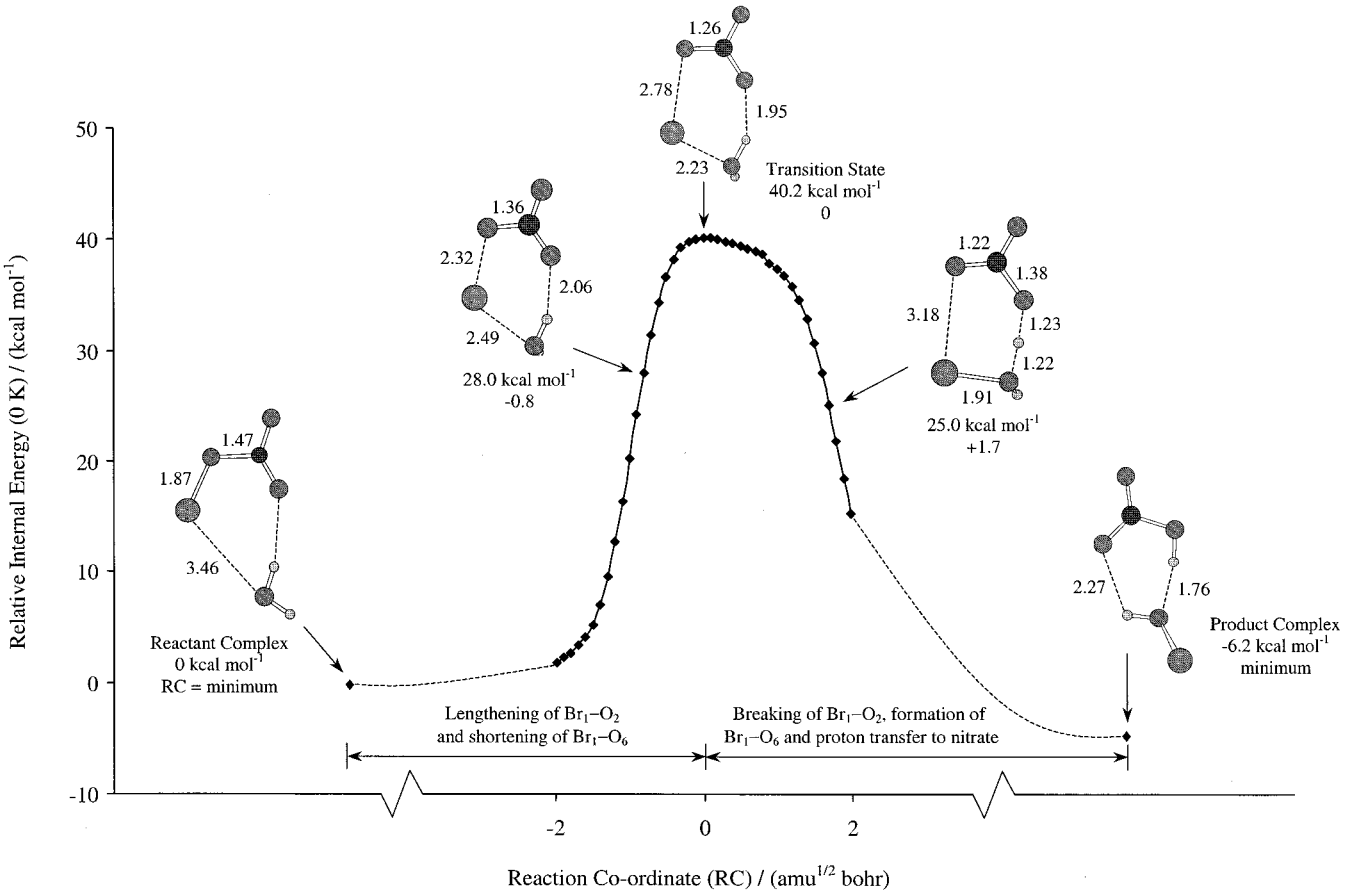

Figure 8. Minimum-energy pathway for $BrONO_2 + (H_2O)$ reaction.

HOCl, where the ion pair is separated by a double layer of water molecules. DFT calculations of the $ClONO_2 + HCl$[73] and $N_2O_5 + H_2O$[67] reactions in analogous ice-like structures also lead to ionic products. In view of these findings and the study by Materer et al.,[56] which found the surface of ice to have complete bilayer termination, we have studied the hydrolysis of $BrONO_2$ in structures related to hexagonal ice.

We have examined two possible structures containing species akin to the $H_2OBr^+NO_3^-$ ion pair. These structures were obtained by separating the ionic species by single and double layers of waters, in line with previous studies.[54,65] Such structures could be formed following the predissociation of $BrONO_2$ such that bromine is transferred to the nucleophilic water, yielding a CIP (Figure 4b) which is subsequently solvated before reaction occurs. These structures can be related to hexagonal ice whereby single and double layers of water molecules can effect ion-pair stabilization.[41,42,67,73] The first such structure, $H_2OBr^+\cdot(H_2O)_3\cdot NO_3^-$ (Figure 5a), contains the ion pair bridged by three water molecules at the apexes of a trigonal bipyramidal structure and is closely related to the $H_2OBr^+\cdot(H_2O)_3\cdot Br^-$ ion pair calculated by Ramondo et al.[54] The H_2OBr entity is distorted from the isolated molecule with a Br_1-O_6 bond length (2.05 Å), somewhat longer than that of the isolated molecule (1.93 Å), possibly due to the interaction of the bromine atom with a second water molecule at a relatively short nonbonded distance of 2.21 Å. Evidence for charge separation is afforded by charges of 0.55 and −0.79 on H_2OBr and NO_3, respectively. The second structure (Figure 5b) differs from the first in that the ion pair is separated by a double layer of water molecules. However, further solvent separation of the ion pair results in only small structural changes. The Br_1-O_6 bond (of H_2OBr) is only a little shorter (2.02 Å) than that in the analogous three-water cluster (Figure 5a), where charges of −0.78 (NO_3) and 0.54 (H_2OBr) are evidence for well-defined nitrate and protonated hypobromous acid (Table 4). In a study of the hydrolysis of Br_2,[54] the $H_2OBr^+\cdot(H_2O)_6\cdot Br^-$ complex is calculated to be some 2 kcal mol^{-1} more stable than the related $H_3O^+\cdot(H_2O)_5\cdot BrOH^-$ structure. However, both the ion pair structures are found to be somewhat less stable than the neutral complex, $Br_2\cdot(H_2O)_7$. Calculations of the hydrolysis of $ClONO_2$ by McNamara and Hillier[42] also find the isomeric structures $H_2OCl^+\cdot NO_3^-\cdot(H_2O)_7$ and $HOCl\cdot H_3O^+\cdot NO_3^-\cdot(H_2O)_6$ to be close in energy.

Having examined the stability of the hypobromous ion and nitrate ion pair, we now turn to the possibility that analogous structures may be stable involving the hypochlorous ion (H_2OCl^+). The formation of H_2OCl^+ in the hydrolysis of chlorine nitrate is somewhat controversial.[36−40] McNamara and Hillier[42] have identified the $H_2OCl^+NO_3^-$ CIP solvated by eight waters at the DFT level; yet some authors argue against the formation of such a species.[45] We have now identified a further two minimum-energy structures on the potential energy surface where the $H_2OCl^+NO_3^-$ ion pair is separated by single and double layers of water molecules. The first (Figure 6a) contains species akin to H_2OCl^+ and NO_3^- and is characterized by a Cl_1-O_6 bond of length 1.88 Å, a little longer than in the isolated molecule (1.77 Å, B3LYP).[42] Further evidence for ion pair formation is afforded by charges of 0.51 and −0.76 on the H_2OCl and NO_3 entities, respectively. A second structure in which the ion pair is separated by a double layer of water molecules has also been identified (Figure 6b) where the structures of the ionic species resemble those in the structure separated by just three water molecules (Figure 6a).

Combined LEED and MD simulations by Materer et al.[56]

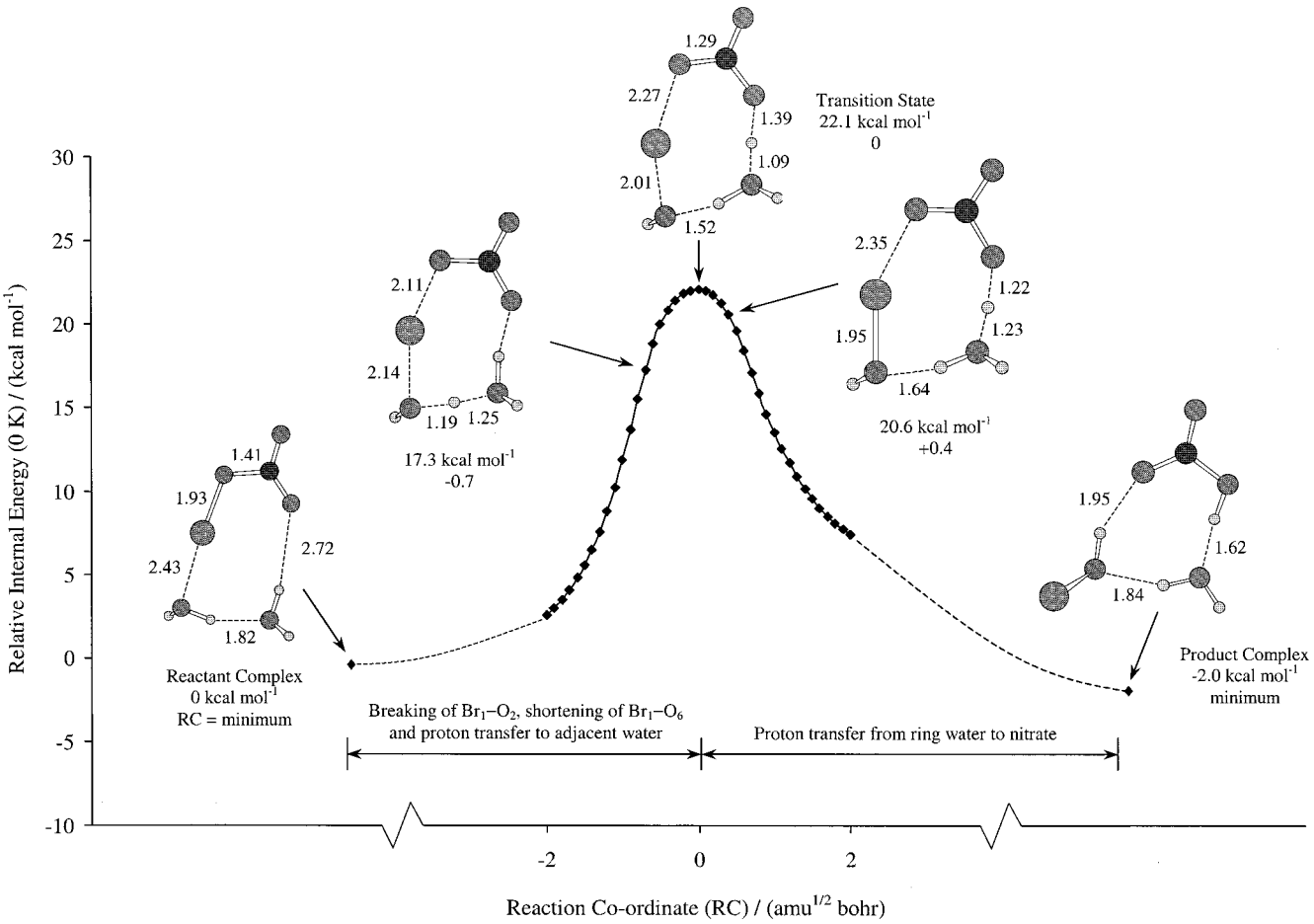

Figure 9. Minimum-energy pathway for $BrONO_2 + (H_2O)_2$ reaction.

suggest that the surface of ice has complete bilayer termination. We have investigated the reactivity of $BrONO_2$ in a six-water cluster generated by replacing two surface bilayer water molecules of such a proton ordered phase of hexagonal ice with a $BrONO_2$ molecule.[41,42,67,73] Energetically, hydrolysis is predicted to be a facile reaction, with an essentially zero barrier (Table 3), a similar barrier being predicted at the MP2 level (0.2 kcal mol^{-1}). Calculations of the hydrolysis of $ClONO_2$ in this six-water structure also indicate a ready reaction on ice, with a barrier of just 0.1 kcal mol^{-1} (Table 3).[41,42] The reactant complex (Figure 7a) is characterized by an increased Br_1-O_2 distance of 2.05 Å and a notably lengthened O_6-H_7 bond of 1.06 Å. Further evidence of ionization (of $BrONO_2$) is supported by a binding energy of 43.3 kcal mol^{-1}, a value greater than those for the structures discussed so far (Table 2). The transition structure (imaginary frequency 259 cm^{-1}, Figure 7b) corresponds to a transfer of Br_1 to H_2O and of H_7 to an adjacent water to form a hydroxonium ion, in line with the proposed hydrolysis mechanism by Bianco and Hynes[45] involving a nucleophilic attack and a coupled proton transfer. We note that the hypobromous ion (H_2OBr^+) is not involved in the hydrolysis MEP we have identified. Importantly, the product structure (Figure 7c) involves the ionized form of nitric acid ($H_3O^+NO_3^-$), where charges of −0.67 (NO_3) and 0.75 (H_3O) are evidence for well-defined nitrate and hydroxonium ions. A strong interaction between HOBr and both nitrate and the hydroxonium ion is also evident, with a relatively short Br_1-O_2 nonbonded distance of 2.24 Å and a charge of −0.16 on HOBr.

C. Vibrational Frequencies. We turn now to consider the correlation of the predicted vibrational frequencies of our model clusters with the available experimental IR data.[35] We first compare our calculated harmonic frequencies for $BrONO_2$ with the gas-phase data[51] and previous high-level calculations.[51,53] Our calculated values are generally in good agreement with the vibrationally averaged gas-phase structure (Table 5), although it can be seen that the CCSD(T)/TZ2P values are somewhat closer to those in the experiment.[51]

At stratospheric conditions (ca. 185 K) the hydrolysis of $BrONO_2$ is believed to occur via an ionic pathway involving the hypobromous ion intermediate (H_2OBr^+).[35] Identification of H_2OBr^+ in the RAIR spectra is made primarily on the assignment of a distinct H_2O deformation mode at 1650 cm^{-1} and the existence of 'perturbed' nitrate absorption features (Table 7) which are attributed to the formation of a contact ion pair (CIP), namely, $H_2OBr^+NO_3^-$. In an IR study of the hydrolysis of $ClONO_2$, Sodeau et al.[38] observe O−H absorptions at ca. 3300 cm^{-1} (broadened by hydrogen-bonding) and a sharp band at 1650 cm^{-1}. These spectral features are readily assigned to the O−H stretching and H_2O deformation modes of the hypochlorous ion (H_2OCl^+) believed to be complexed with nitrate,[36−40] although other calculations have assigned this peak to molecular nitric acid.[45,86]

Comparison between the calculated vibrational frequencies for our cluster models and the available IR data[35] can reveal details at a molecular level of the role of the ice surface in solvating key ionic species. We first consider the ring structures (Figures 1−4) related to the rings of waters reported on the ice surface by Buch et al.[61] A central feature of this study that has been implicated thus far by our ring structures is the importance of predissociation or ionization along the $Br-ONO_2$ bond, serving to increase the electrophilicity of the bromine atom. During ionization and transfer of the bromine atom, there is an

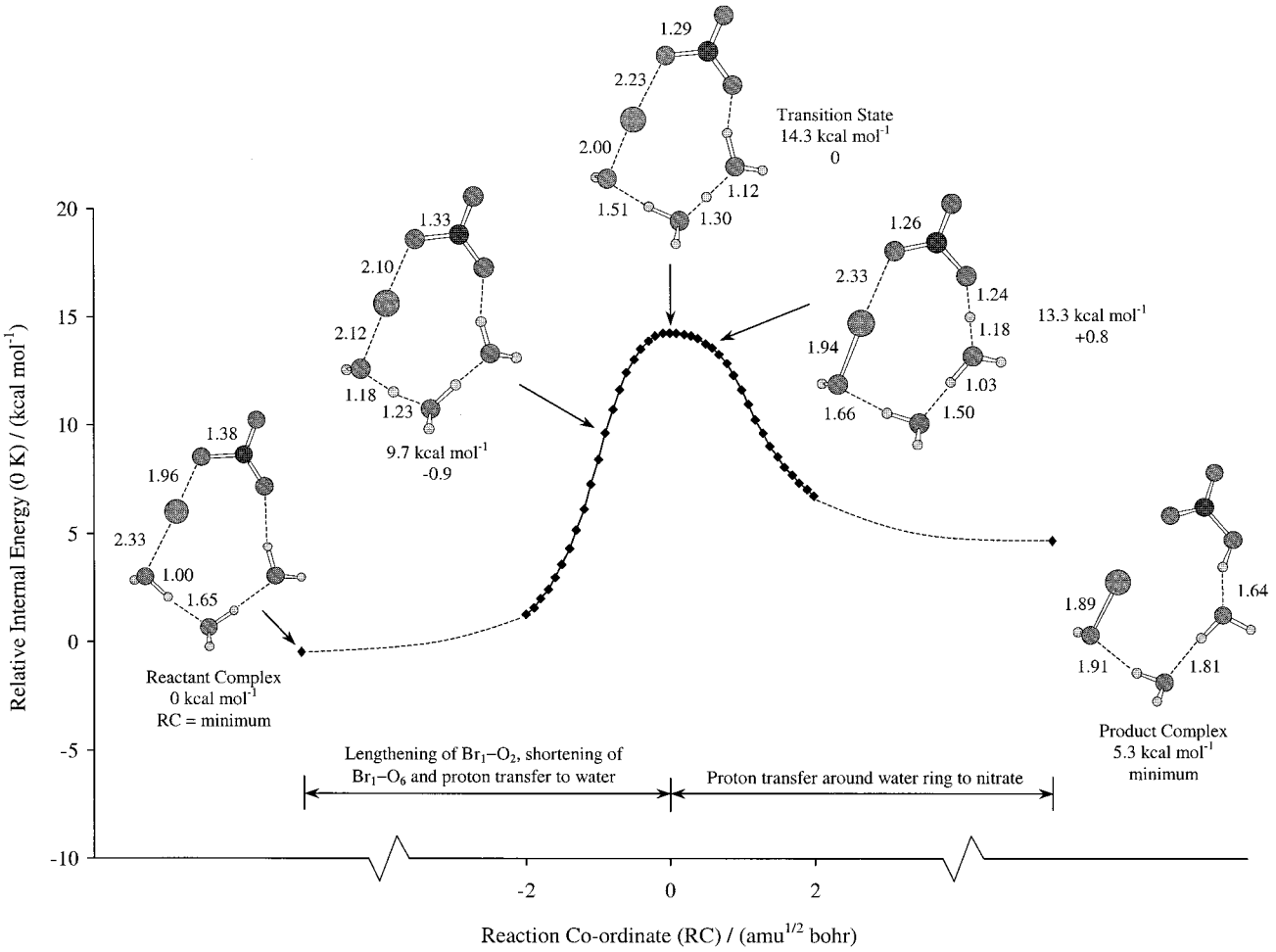

Figure 10. Minimum-energy pathway for $BrONO_2 + (H_2O)_3$ reaction.

associated lengthening of the O−H bonds of the attacking water molecule. As a result, we observe a lowering of the calculated O−H stretching frequency of the nucleophilic water (Table 6). Gane and Sodeau[35] have recorded an IR spectrum of $BrONO_2$ dosed onto a thin film of water ice, annealed at 140 K (Table 6). The reported vibrational frequencies (Table 6) are close to those for gas-phase $BrONO_2$ (Table 5), indicating that no reaction has taken place. In line with experiment, the calculated vibrational frequencies for $BrONO_2$ solvated by up to six waters (Table 6) are close to those for the free molecule (Table 5). This finding suggests that the ring structures (Figures 1−4) may be structurally close to the annealed ice film (140 K) containing unreactive $BrONO_2$. In contrast, we have identified an eight-water cluster (Figure 4b) in which the bromine atom is closer to the attacking nucleophile than to the departing nitrate [Br_1-O_2 2.13 Å, Br_1-O_6 2.08 Å] and thus resembles a $H_2OBr^+NO_3^-$ contact ion pair. However, we see that the predicted vibrational frequencies (Table 6) mirror those of free $BrONO_2$ (Table 5). Experimentally, the formation of H_2OBr^+ (Table 7) results in absorption bands quite different from those of $BrONO_2$ (Table 5), suggesting that the observed ionic species[35] may not involve a CIP but rather a solvent separated ion pair. We now discuss the calculated vibrational frequencies for the structures containing the ion pairs $H_2OBr^+NO_3^-$ (Figure 5) and $H_2OCl^+NO_3^-$ (Figure 6) separated by single and double layers of water molecules.

For the complex involving three-water molecules (Figure 5a), solvation of the H_2OBr^+ entity results in a lengthening of the O−H bonds, which is reflected in a shift to lower frequency of the O−H stretching vibrations by some 700 cm^{-1} (Table 7) compared to that in the free molecule case (Table 7). Furthermore, hydration (of H_2OBr^+) leads to an increased Br−O distance of 2.05 Å (1.93 Å, free molecule),[42] which, as expected, leads to a shift to lower frequency of the Br−O stretching vibration (Table 7).[35] The identification of H_2OBr^+ in RAIR experiments[35] is made primarily on the assignment of the distinct H_2O deformation mode observed at 1650 cm^{-1}, predicted to occur at 1730 cm^{-1} in this structure. Notably, solvent separation of the ion pair results in a lifting of the degeneracy of the NO_3 asymmetric stretching vibration with two components calculated at 1415 and 1374 cm^{-1}, and the NO_3 symmetric stretching vibration, formerly forbidden for a symmetric nitrate, is calculated to have a low intensity at 1081 cm^{-1}, in line with experimental observations.[35] For the ion pair structure separated by a double layer of water molecules (Figure 5b), we predict a further lowering of the O−H stretching vibrations of H_2OBr^+ by ca. 900 cm^{-1} compared to that in the isolated molecule. The most intense of the calculated H_2O deformation modes (Table 7) for this structure occurs at 1650 cm^{-1}, close to those in the experiment (Table 7). Evidently, the H_2O deformation mode does not change much with the number of solvating waters and is therefore more representative of the nature of the ionic species (H_2OBr^+) than the O−H stretching modes, which show large shifts on increased solvation.[54]

In view of the good agreement between the calculated and experimental vibrational frequencies for structures involving H_2-

TABLE 4: Mulliken Charges (e) of $BrONO_2$ Hydrolysis Structures

		atomic charges								total fragment charges: reactants		intermediates			products			
structure[a]		Br_1	O_2	N_3	O_4	O_5	O_6	H_7	H_8	$BrONO_2$	H_2O	H_2OBr	H_3O	NO_3	H_3O	NO_3	HOBr	$HONO_2$
Ring Clusters																		
$BrONO_2 \cdot (H_2O)$[b]	R	0.20	0.03	−0.28	0.03	0.03	−0.52	0.26	0.25	0.01	−0.01							
	TS	0.12	−0.03	−0.23	−0.02	−0.17	−0.34	0.31	0.36	−0.33	0.33	0.45		−0.45				
	P	0.14	−0.07	−0.25	0.01	−0.07	−0.43	0.27	0.40								−0.02	0.02
$BrONO_2 \cdot (H_2O)_2$[c]	R	0.21	−0.01	−0.30	0.00	−0.03	−0.50	0.35	0.29	−0.13	0.14							
	TS	0.13	−0.04	−0.31	−0.02	−0.19	−0.57	0.41	0.30	−0.43	0.14		0.70	−0.56				
	P	0.13	−0.09	−0.29	0.00	−0.06	−0.43	0.35	0.30								0.00	−0.01
$BrONO_2 \cdot (H_2O)_3$[d]	R	0.23	−0.02	−0.32	0.00	−0.07	−0.53	0.38	0.29	−0.18	0.14							
	TS	0.14	−0.06	−0.31	−0.04	−0.20	−0.61	0.41	0.29	−0.47	0.09		0.69	−0.61				
	P	0.13	−0.05	−0.29	0.01	−0.06	−0.46	0.34	0.28								−0.05	0.03
$BrONO_2 \cdot (H_2O)_5$[e]		0.18	−0.05	−0.32	−0.02	−0.10	−0.55	0.40	0.39	−0.31	0.24							
$BrONO_2 \cdot (H_2O)_6$[f]		0.18	−0.06	−0.32	−0.02	−0.10	−0.56	0.41	0.39	−0.32	0.24							
$BrONO_2 \cdot (H_2O)_8$[g]		0.18	−0.13	−0.29	−0.03	−0.14	−0.55	0.45	0.42	−0.41	0.32	0.50		−0.59				
Ice-Like Clusters																		
$H_2OBr^+ \cdot (H_2O)_3 \cdot NO_3^-$[h]		0.21	−0.07	−0.56	−0.07	−0.09	−0.44	0.40	0.38			0.55		−0.79				
$H_2OBr^+ \cdot (H_2O)_6 \cdot NO_3^-$[i]		0.19	−0.09	−0.35	−0.16	−0.18	−0.51	0.42	0.44			0.54		−0.78				
$BrONO_2 \cdot (H_2O)_6$[j]	R	0.22	−0.01	−0.39	0.02	−0.17	−0.54	0.46	0.30	−0.33	0.22							
	TS	0.19	−0.03	−0.37	0.00	−0.22	−0.61	0.51	0.29	−0.43	0.19			−0.62				
	P	0.16	−0.06	−0.34	−0.02	−0.25	−0.61	0.48	0.29						0.74	−0.67	−0.16	

[a] Refer to Figure 1a for atom labeling. R (reactants), TS (transition state), and P (products). [b] Figure 1. [c] Figure 2. [d] Figure 3. [e] Figure 4a. [f] Figure 4a solvated at A. [g] Figure 4b. [h] Figure 5a. [i] Figure 5b. [j] Figure 7.

TABLE 5: Experimental and Calculated Vibrational Frequencies (cm^{-1}) and (in Parentheses) Intensities (km mol^{-1}) for $BrONO_2$

assignment	experiment[a]	B3LYP/6-311++G(d,p)	B3LYP/TZ2P[b]	MP2/6-311G(d)[c]	CCSD(T)/TZ2P[d]
NO_2 asym str	1714 (vs)	1768 (368)	1743 (353)	1951	1708 (325)
NO_2 sym str	1288 (vs)	1331 (312)	1321 (297)	1319	1291 (272)
NO_2 sciss	803.3 (vs)	817 (217)	818 (204)	795	814 (204)
BrO str + NO_2 sciss	750 (w)	743 (2)	747 (5)	739	745(2)
NO_3 op bend	728 (wm)	733 (10)	744 (11)	723	721 (9)
ON str	564 (s)	548 (102)	560 (93)	502	562 (85)
NO_2 sciss + BrO str	394	391 (2)	393 (4)	383	389 (2)
BrON bend		202 (0.03)	209 (0.04)	212	215 (0.01)
torsion		113 (0.5)	112 (0.3)	112	100 (0.03)

[a] Parthiban and Lee[51] and references therein. [b] Parthiban and Lee.[53] [c] Ying and Zhao.[52] [d] Parthiban and Lee.[51]

OBr^+, we have also calculated the values for analogous structures involving H_2OCl^+ (Figure 6a,b). Solvation of the H_2OCl^+ entity also results in a lowering of the O−H stretching frequencies by up to 1150 cm^{-1} (six-waters) compared to that in the free molecule (Table 7). The calculated H_2O deformation frequencies of these structures also correlate well with those in the experiment (Table 7).

Finally, we turn now to a discussion of the structure containing both HOBr and ionized nitric acid ($H_3O^+NO_3^-$, Figure 7c), where the ionic species are separated by a double layer of water molecules. We see that the predicted vibrational frequencies (Table 7) for both H_3O^+ and NO_3^- more closely resemble those observed for NAD[35] than for NAT, which is expected since both ionic species are solvated by two-water molecules.

5. Discussion

We first comment on the method of including electron correlation and the choice of basis set. Our calculations have shown that DFT (B3LYP functional), combined with the flexible 6-311++G(d,p) basis, correctly describes the structure of $BrONO_2$ itself (Table 1) and is in good agreement with both the higher-level calculations (MP2[83] and CCSD(T)[51,53]) and electron diffraction data.[82]

The calculations described herein reveal a number of important features concerning the hydrolysis of $BrONO_2$ in small water clusters and on PSC ice aerosols. Gane and Sodeau[35] report two alternative reaction pathways. At stratospheric conditions (ca. 185 K), the reaction proceeds by an ionic mechanism, whereas a molecular mechanism is favored at lower temperatures (ca. 140 K) and reduced water conditions. We now

TABLE 6: Experimental and Calculated Vibrational Frequencies (cm^{-1}) and Intensities (km mol^{-1}) of Reactant Structures

		rings						ice-like
assignment	experiment[a]	$BrONO_2$ $\cdot(H_2O)$[b]	$BrONO_2$ $\cdot(H_2O)_2$[c]	$BrONO_2$ $\cdot(H_2O)_3$[d]	$BrONO_2$ $\cdot(H_2O)_5$[e]	$BrONO_2$ $\cdot(H_2O)_6$[f]	$BrONO_2$ $\cdot(H_2O)_8$[g]	$BrONO_2$ $\cdot(H_2O)_6$[h]
				$BrONO_2$				
NO_2 asym str	1655	1751 (407)	1687 (384)	1660 (315)	1625 (457)	1616 (440)	1581 (371)	1593 (507)
NO_2 sym str	1270	1327 (299)	1311 (358)	1307 (412)	1302 (494)	1301 (514)	1300 (548)	1279 (128)
								1268 (465)
NO_2 deform	816	825 (203)	857 (243)	893 (306)	930 (326)	938 (330)	979 (277)	976 (251)
BrO str	741	746 (2)	749 (30)	749 (25)	740 (82)	741 (23)	746 (26)	757 (59)
								736 (11)
NO_3 op bend	727	734 (11)	759 (11)	764 (10)	776 (9)	778 (8)	799 (20)	797 (19)
					747 (52)			
				H_2O[i]				
O−H str	3300	3912 (110)	3855 (127)	3849 (116)	3290 (1626)	3314 (1410)	3054 (1826)	2206 (3079)
		3806 (28)	3514 (62)	3178 (1345)	3191 (1289)	2930 (2135)	2623 (2819)	3831 (132)
H_2O deform		1600 (60)	1635 (52)	1676 (33)	1676 (27)	1689 (19)	1634 (28)	1727 (34)
			1620 (76)	1647 (178)	1659 (49)	1658 (60)		1692 (37)
				1633 (71)	1646 (51)	1636 (24)		
					1633 (31)			

[a] RAIR spectra of $BrONO_2$ dosed onto thin film of water-ice and annealed to 140 K (*unreactive*).[35] [b] Figure 1a. [c] Figure 2a. [d] Figure 3a. [e] Figure 4a. [f] Figure 4a solvated at A. [g] Figure 4b. [h] Figure 7a. [i] Nucleophile.

TABLE 7: Experimental and Calculated Vibrational Frequencies (cm^{-1}) and (in parentheses) Intensities (km mol^{-1}) of Ice-like (ion pair) Structures

assignment	experiment		free[c]		ion pair structure			
H_2OX^+	Br[a]	Cl[b]	Br	Cl	H_2OBr^+ $\cdot(H_2O)_3\cdot NO_3^-$ [e]	H_2OBr^+ $\cdot(H_2O)_6\cdot NO_3^-$ [f]	H_2OCl^+ $\cdot(H_2O)_3\cdot NO_3^-$ [g]	H_2OCl^+ $\cdot(H_2O)_6\cdot NO_3^-$ [h]
O−H str	3360 (br)	3350	3679 (386)	3625 (420)	2988 (2294)	2774 (2879)	2688 (1624)	2505 (2855)
			3590 (356)	3540 (339)	2908 (415)	2676 (2309)	2490 (1711)	2378 (2877)
					2827 (1065)	2644 (1972)		
H_2O deform	1650 (m)	1650	1609 (83)	1614 (89)	1730 (98)	1717 (6)	1733 (99)	1719 (17)
						1691 (31)		1703 (92)
						1650 (119)		1692 (43)
								1645 (73)
XOH deform			941 (9)	1037(8)	1294(164)	1313 (70)	1313 (72)	1388 (56)
			722 (218)	808 (206)	1206 (37)	1209 (169)	1428 (160)	1276 (118)
X−O str			536 (26)	624 (55)	447 (32)	499 (52)	520 (130)	541 (34)
NO_3^-								
NO_3 asym str	1508 (s)	1430	1377 (600)		1415 (423)	1448 (367)	1398 (348)	1455 (370)
	1335 (s)	1350	1377 (601)		1374 (351)	1368 (519)	1380 (413)	1361 (537)
NO_3 sym str	1035 (m)	1040	1065 (0)		1081 (5)	1076 (17)	1083 (3)	1073 (21)
NO_3 op bend			835 (8)		849 (74)	827 (80)	831 (40)	846 (104)
					855 (112)			
NO_3 deform	806 (m)	820	709 (0.05)		717 (65)	732 (14)	725 (8)	732 (12)
			709 (0.05)					
H_3O^+	NAD[d]	NAT[d]	$HOBr\cdot H_3O^+\cdot(H_2O)_4\cdot NO_3^-$ [i]					
O−H str	2814 (br)	2900 (br)	3678 (499)		2905 (889)			
	2300 (br)		3678 (498)		2727 (2313)			
			3581 (40)		2271 (2752)			
H_2O deform	1750(vw)	1750 (vw)	1674 (121)		1778 (7)			
			1673 (121)		1743 (9)			
H_3O deform	1182(vs)	1136 (s)			1069 (51)			
H_3O op bend			766 (518)		1376 (335)			
NO_3^-								
N═O str	1457 (m)	1364 (m)			1534 (604)			
NO_2 asym str	1267 (m)				1264 (627)			
NO_2 sym str	1023 (vw)				1052 (89)			
NO_3 deform	808 (s)	821 (vs)			826 (23)			
HOBr								
O−H str	2596		3788 (91)		3828 (114)			
BrOH deform			1149 (39)		1069 (51)			
Br−O			605 (8)		461 (118)			

[a] RAIR spectra of $BrONO_2$ codeposited with H_2O (50:1) at 185 K on gold substrate.[35] [b] FT-RAIR spectra of $ClONO_2$ codeposited with water (10:1) at 180 K on gold substrate.[38] [c] Calculated at the B3LYP/6-311++G(d,p) level. [d] Gane and Sodeau.[35] [e] Figure 5a. [f] Figure 5b. [g] Figure 6a. [h] Figure 6b. [i] Figure 7c.

discuss the relevance of our calculations to the proposed hydrolysis mechanisms.

The hydrolysis of $BrONO_2$ at low temperatures (140 K) yields the molecular products $HONO_2$ and HOBr [reaction 1][35] and is in line with $ClONO_2$ hydrolysis at this temperature [$HONO_2$ and HOCl, reaction 2].[40] Some authors point to the inability of $XONO_2$ (X = Cl, Br) to pre-ionize at lower temperatures as a reason for the observed molecular reaction pathway.[35,39,40] Hydrolysis (of $BrONO_2$) in the clusters containing one-, two-, and three-water molecules (Figures 1a, 2a, and 3a) leads to reaction products involving the molecular acids ($HONO_2$ and HOBr), and these clusters may be appropriate to hydrolysis at 140 K. In the one-water reaction, the reactant cluster (Figure 1a) contains un-ionized $BrONO_2$, where the MEP is character-

ized by an S_N2 attack of water at Br_1 leading to a six-membered ring TS-containing[85] species akin to $H_2OBr^+NO_3^-$. The barrier (42.4 kcal mol^{-1}) is less than for $ClONO_2$ hydrolysis (48.8 kcal mol^{-1})[43] but is too high to account for the expected ready reaction on ice.[87] For the two- (Figures 2 and 9) and three-water catalyzed reactions (Figures 3 and 10), the reactant clusters each contain $BrONO_2$ molecules with Br_1-O_2 bonds (1.93 and 1.96 Å) a little longer than those in the free molecule (1.87 Å, B3LYP). In line with the one-water catalyzed reaction, the MEPs are characterized by S_N2 attack of water at Br_1 and a coupled proton transfer,[45] leading to TS structures where the positive charge is now located on species close to H_3O^+. The energy barriers are notably lower than those for the one-water catalyzed reaction, being 22.1 (two-water) and 13.4 kcal mol^{-1} (three-water), values close to those for hydrolysis of $ClONO_2$ in such clusters (22.4 and 14.5 kcal mol^{-1}, Table 3),[43] showing the catalytic effect of increasing the size of the water cluster. The two- and three-water clusters we have considered can be related to fragments excised from the ideal ice surface, but in each of these structures, the developing nitrate is only solvated at O_5, and thus, the water cluster is unable to effect ionization (of $BrONO_2$). Thus, the molecular pathway is expected to proceed as reaction 1. Solvation of O_2 of the incipient nitrate group in the three-water reactant cluster (Figure 3a) by two additional water molecules leads to a five-water cluster (Figure 4a) in which $BrONO_2$ is somewhat ionized. An increased Br_1-O_2 distance (2.03 Å) and binding energy (35.4 kcal mol^{-1}) compared to those for the three-water clusters (1.96 Å and 22.0 kcal mol^{-1}) are evidence of a change toward an ionic mechanism. Further hydration of these structures, particularly of the incipient nitrate group, facilitates ionization along the $Br-ONO_2$ bond, thus favoring the ionic reaction.[41,42] This has been shown to be the case for the hydrolysis of $ClONO_2$.[41,42]

At stratospherically relevant conditions (185 K), the heterogeneous hydrolysis of $BrONO_2$ is postulated to involve the hypobromous acid ion (H_2OBr^+) under limited water conditions. The formation of protonated acids in halogen hydrolysis is somewhat controversial. Bell and Gelles[88] have observed H_2OX^+ (X = Cl, Br, and I), whereas Eigen and Kustin[89] appear to rule out the formation of such species in aqueous solution studies of $X_2 + H_2O \rightarrow XOH + H^+ + X^-$. More recently, Ramondo and Sodeau report reaction pathways involving the $H_2OBr^+\cdot(H_2O)_n\cdot Br^-$ ion pair in RAIRS studies of Br_2 hydrolysis, which are competitive with routes occurring via an H_3O^+ ion,[54] while the hypochlorous ion (H_2OCl^+) is implicated in the hydrolysis of $ClONO_2$.[36-42] Ab initio calculations predict both the H_2OCl^+ [42] and H_2OBr^+ [54] ions to be stable in small water clusters where the most stable isomer involves protonation of oxygen.[55,90,91] However, quantum chemical calculations[45] of the $ClONO_2$ hydrolysis pathway do not involve the H_2OCl^+ intermediate, and recent calculations and analysis of the available spectroscopic data argue against the formation of H_2OCl^+.[86]

Identification of H_2OBr^+ in RAIRS experiments is made primarily on the assignment of the distinct H_2O deformation mode measured at 1650 cm^{-1}.[35] The calculated vibrational frequencies for our eight-water cluster (Figure 4b) containing species akin to the $H_2OBr^+NO_3^-$ CIP are close to those for free $BrONO_2$ at this level (B3LYP). This is not unexpected given a relatively short intermolecular Br_1-O_2 distance (2.14 Å), indicating a strong interaction between nitrate and Br_1. However, the reported RAIR spectra of H_2OBr^+ are somewhat different from that of unreactive $BrONO_2$ dosed onto a thin film of water ice, suggesting that H_2OBr^+ may not form a CIP with nitrate. We have thus re-examined our calculations of an analogous eight-water cluster containing the $H_2OCl^+NO_3^-$ CIP.[42] The calculated vibrational frequencies also mirror those of isolated $ClONO_2$, but we note that the reported H_2O deformation mode (1408 cm^{-1}) actually corresponds to the ClOH bending vibration, whereas the H_2O deformation mode is predicted at 1635 cm^{-1} for this structure. The calculated vibrational frequencies for structures containing both the protonated acid (H_2OBr^+ or H_2OCl^+, Figures 5 and 6) and nitrate, separated by single and double layers of waters, correlate well with experiment (Table 7), which suggests the formation of a solvent separated ion pair. The calculations predict the O-H stretching frequencies of hydrated H_2OBr^+ (ca. 2600 cm^{-1}) to be somewhat lower than those in the free molecule (ca. 3500 cm^{-1}) and experiment (ca. 3300 cm^{-1}). However, the calculations are in good agreement with RAIRS studies of the hydrolysis of Br_2, which report the O-H stretching vibrations of H_2OBr^+ at 2900 and 3300 cm^{-1}, respectively. The calculated vibrational frequencies for the three- and six-water clusters containing H_2OBr^+ imply that the O-H stretching frequencies of H_2OBr^+ are strongly dependent on the solvating environment, whereas the H_2O deformation frequency changes little (Table 7).[54]

We turn now to consider the hydrolysis of $BrONO_2$ in a cluster where the arrangement of the water molecules is structurally related to hexagonal ice.[41,42,67,73] The MEP (not shown) proceeds from a reactant structure (Figure 7a) containing strongly ionized $BrONO_2$, leading to reaction products (Figure 7c) containing the ionic ($H_3O^+NO_3^-$) and molecular acids (HOBr). In line with the structures containing $H_2OBr^+NO_3^-$ (Figure 5) or $H_2OCl^+NO_3^-$ (Figure 6), this structure involves both H_3O^+ and NO_3^- separated by a double layer of water molecules. The calculated barrier (Table 3, B3LYP) indicates an essentially spontaneous reaction under stratospheric conditions, with a similar barrier being predicted for the hydrolysis $ClONO_2$ in this cluster (Table 3).[41,42] The reaction mechanism involves nucleophilic attack of water at the bromine atom (of $BrONO_2$) coupled with a proton transfer to an adjacent water molecule, supporting the mechanism proposed by Bianco and Hynes.[45]

In summary, our investigations have revealed at a molecular level, details of both the molecular and ionic hydrolysis pathways for $XONO_2$ (X = Cl, Br). The molecular pathway involves only partial solvation of the developing nitrate, thus leading to the molecular acid products ($HONO_2$ and XOH). In contrast, the ionic mechanism involves significant ionization (or predissociation) of $XONO_2$ in the reactant cluster and may lead to the formation of the $H_2OX^+NO_3^-$ CIP in the extreme case. Further solvation of the ionic species may result in the solvent separation of the ion pair yielding $H_2OX^+\cdot(H_2O)_n\cdot NO_3^-$, which collapses to form the ionic products ($H_3O^+NO_3^-$ and XOH). However, the exact details of the hydrolysis mechanism will be strongly dependent on the nature of the ice surface and, particularly, the availability of additional solvating waters at the PSC surface. In clusters related to hexagonal ice, the hydrolysis of $BrONO_2$ is predicted to be essentially spontaneous. Our range of model clusters have accounted for a number of different absorption sites likely to be found on the PSC ice aerosol surface. However, our central finding of atmospheric importance[1-8] is that the hydrolysis of $XONO_2$ (X = Cl, Br) can proceed essentially spontaneously in neutral water clusters of a relatively small critical size (via ionic pathways) that do not require larger aerosols or clusters containing solvated ionic species.[8]

Acknowledgment. We thank EPSRC and NERC for support of this research and Professor J. Sodeau for a preprint of ref 35.

References and Notes

(1) Soloman, S. *Rev. Geophys.* **1988**, *26*, 131.
(2) Soloman, S.; Garcia, R. R.; Rowland, F. S.; Wuebbles, D. J. *Nature* **1986**, *321*, 755.
(3) Soloman, S.; Portmann, R. W.; Garcia, R. R.; Thomason, L. W.; Poole, L. R.; McCormick, M. R. *J. Geophys. Res.* **1996**, *101*, 6713.
(4) Henderson, G. S.; Evans, W. F. J.; McConnell, J. C. *J. Geophys. Res.* **1990**, *95*, 1899.
(5) Soloman, S. *Nature* **1990**, *347*, 347.
(6) Turco, R. P.; Toon, O. B.; Hamill, P. *J. Geophys. Res.* **1989**, *94*, 16493.
(7) Cicerone, R. J. *Science* **1987**, *237*, 35.
(8) Crutzen, P. J.; Arnold, F. *Nature* **1986**, *324*, 651.
(9) Wennberg, P. O.; Cohen, R. C.; Stimpfle, R. M.; Koplow, J. P.; Anderson, J. G.; Salawitch, R. J.; Fahey, D. W.; Woodbridge, E. L.; Keim, E. R.; Gao, R. S.; Webster, C. R.; May, R. D.; Toohey, D. W.; Avallone, L. M.; Proffitt, M. H.; Loewenstein, M.; Podolske, J. R.; Chan, K. R.; Wofsy, S. C. *Science* **1994**, *266*, 398.
(10) Molina, M. J.; Tso, T.-L.; Molina, L. T.; Wang, F. C.-Y. *Science* **1987**, *238*, 1253.
(11) Molina, M. J.; Rowland, F. S. *Nature* **1974**, *249*, 810.
(12) Wofsy, S. C.; McElroy, M. B.; Yung, Y. L. *Geophys. Res. Lett.* **1975**, *2*, 215.
(13) Tie, X. X.; Brasseur, G. *Geophys. Res. Lett.* **1996**, *23*, 2505.
(14) McConnell, J. C.; Henderson, G. S.; Barrie, L.; Bottenheim, J.; Niki, H.; Langford, C. H.; Templeton, E. M. J. *Nature* **1992**, *355*, 150.
(15) Dickerson, R. R.; Rhoads, K. P.; Carsey, T. P.; Oltmans, S. J.; Burrows, J. P.; Crutzen, P. J. *J. Geophys. Res.* **1999**, *104*, 21385.
(16) Randeniya, L. K.; Vohralik, P. F.; Plumb, I. C.; Ryan, K. R.; Baughcum, S. L. *Geophys. Res. Lett.* **1996**, *23*, 1633.
(17) Lary, D. J. *J. Geophys. Res.* **1996**, *101*, 1505.
(18) Lary, D. J.; Chipperfield, M. P.; Toumi, R.; Lenton, T. *J. Geophys. Res.* **1996**, *101*, 1489.
(19) *Scientific Assessment of Ozone Depletion*; World Meteorological Organisation, Global Ozone Research and Monitoring Project - Report 44; World Meteorological Organization:1998. (http://www.wmo.ch).
(20) Burkholder, J. B.; Ravishankara, A. R.; Soloman, S. *J. Geophys. Res.* **1995**, *100*, 16793.
(21) Spencer, J. E.; Rowland, F. S. *J. Phys. Chem.* **1978**, *82*, 7.
(22) Deters, B.; Burrows, J. P.; Orphal, J. *J. Geophys. Res.* **1998**, *103*, 3563.
(23) Fan, S.-M.; Jacob, D. J. *Nature* **1992**, *359*, 522.
(24) Hanson, D. R.; Ravishankara, A. R. *Geophys. Res. Lett.* **1995**, *22*, 385.
(25) Allanic, A.; Oppliger, R.; Rossi, M. J. *J. Geophys. Res.* **1997**, *102*, 23529.
(26) Hanson, D. R.; Ravishankara, A. R.; Lovejoy, E. R. *J. Geophys. Res.* **1996**, *101*, 9063.
(27) Hanson, D. R.; Ravishankara, A. R. *J. Geophys. Res.* **1991**, *96*, 5081.
(28) Leu, M.-T. *Geophys. Res. Lett.* **1988**, *15*, 17.
(29) Hanson, D. R.; Ravishankara, A. R. *J. Phys. Chem.* **1992**, *96*, 2682.
(30) Hanson, D. R.; Ravishankara, A. R. *J. Geophys. Res.* **1991**, *96*, 17307.
(31) Hanson, D. R. *J. Phys. Chem. A* **1998**, *102*, 4794.
(32) Hanson, D. R.; Ravishankara, A. R. *J. Phys. Chem.* **1994**, *98*, 5728.
(33) Zhang, R.; Jayne, J. T.; Molina, M. J. *J. Phys. Chem.* **1994**, *98*, 867.
(34) Zhang, R.; Leu, M.-T.; Keyser, L. *J. Phys. Chem.* **1994**, *98*, 13563.
(35) Gane, M. P.; Sodeau, J. R. *J. Phys. Chem. A* **2001**, *105*, 4002.
(36) Banham, S. F.; Horn, A. B.; Koch, T. G.; Sodeau, J. R. *J. Chem. Soc., Faraday Discuss.* **1995**, *100*, 321.
(37) Sodeau, J. R.; Horn, A. B.; Banham, S. F.; Kock, T. G. *J. Phys. Chem.* **1995**, *99*, 6258.
(38) Koch, T. G.; Banham, S. F.; Sodeau, J. R.; Horn, A. B.; McCoustra, M. R. S.; Chesters, M. A. *J. Geophys. Res.* **1997**, *102*, 1513.
(39) Horn, A. B.; Sodeau, J. R.; Roddis, T. B.; Williams, N. A. *J. Phys. Chem. A* **1998**, *102*, 6107.
(40) Horn, A. B.; Sodeau, J. R.; Roddis, T. B.; Williams, N. A. *J. Chem. Soc., Faraday Trans.* **1998**, *94*, 1721.
(41) McNamara, J. P.; Tresadern, G.; Hillier, I. H. *Chem. Phys. Lett.* **1999**, *310*, 265.
(42) McNamara, J. P.; Hillier, I. H. *J. Phys. Chem. A* **1999**, *103*, 7310.
(43) McNamara, J. P.; Hillier, I. H. *Chem. Phys. Lett.* **2000**, *328*, 492.
(44) Akhmatskaya, E. V.; Apps, C. J.; Hillier, I. H.; Masters, A. J.; Palmer, I. J.; Watt, N. E.; Vincent, M. A.; Whitehead, J. C. *J. Chem. Soc., Faraday Trans.* **1997**, *93*, 2775.
(45) Bianco, R.; Hynes, J. T. *J. Phys. Chem. A* **1998**, *102*, 309.
(46) Xu, S. C.; Zhao, X. S. *Acta Phys.-Chim. Sin.* **1998**, *14*, 988.
(47) Xu, S. C.; Zhao, X. S. *J. Phys. Chem. A* **1999**, *103*, 2100.
(48) Ying, L.; Zhao, X. S. *J. Phys. Chem. A* **1997**, *101*, 6807.
(49) Lee, T. J.; Rice, J. E. *J. Phys. Chem.* **1993**, *97*, 6637.
(50) Lee, T. J. *J. Phys. Chem.* **1995**, *99*, 1943.
(51) Parthiban, S.; Lee, T. J. *J. Chem. Phys.* **1998**, *109*, 525.
(52) Ying, L.; Zhao, X. S. *J. Phys. Chem. A* **1997**, *101*, 3569.
(53) Parthiban, S.; Lee, T. J. *J. Chem. Phys.* **2000**, *113*, 145.
(54) Ramondo, F.; Sodeau, J. R.; Roddis, T. B.; Williams, N. A. *Phys. Chem. Chem. Phys.* **2000**, *2*, 2309.
(55) Lee, T. J.; Francisco, J. S. *Chem. Phys. Lett.* **1996**, *251*, 400.
(56) Materer, N.; Starke, U.; Barbieri, A.; Van Hove, M. A.; Somorjai, G. A.; Kroes, G.-J.; Minot, C. *J. Phys. Chem.* **1995**, *99*, 6267.
(57) Silva, S. C.; Devlin, J. P. *J. Phys. Chem.* **1994**, *98*, 10847.
(58) Devlin, J. P.; Buch, V. *J. Phys. Chem.* **1995**, *99*, 16534.
(59) Devlin, J. P.; Buch, V. *J. Phys. Chem. B* **1997**, *101*, 6095.
(60) Rowland, B.; Kadagathur, N. S.; Devlin, J. P.; Buch, V.; Feldman, T.; Wojcik, M. J. *J. Phys. Chem.* **1995**, *99*, 8328.
(61) Buch, V.; Delzeit, L.; Blackledge, C.; Devlin, J. P. *J. Phys. Chem.* **1996**, *100*, 3732.
(62) Geiger, F. M.; Hicks, J. M.; de Dios, A. C. *J. Phys. Chem. A* **1998**, *102*, 1514.
(63) Robinson Brown, A.; Doren, D. J. *J. Phys. Chem. B* **1997**, *101*, 6308.
(64) Vincent, M. A.; Palmer, I. J.; Hillier, I. H.; Akhmatskaya, E. V. *J. Am. Chem. Soc.* **1998**, *120*, 3431.
(65) Smith, A.; Vincent, M. A.; Hillier, I. H. *J. Phys. Chem. A* **1999**, *103*, 1132.
(66) Larson, L. J.; Kuno, M.; Tao, F.-M. *J. Chem. Phys.* **2000**, *112*, 8830.
(67) McNamara, J. P.; Hillier, I. H. *J. Phys. Chem. A* **2000**, *104*, 5307.
(68) Hanway, D.; Tao, F.-M. *Chem. Phys. Lett.* **1998**, *285*, 459.
(69) Snyder, J. A.; Hanway, D.; Mendez, J.; Jamka, A. J.; Tao, F.-M. *J. Phys. Chem. A* **1999**, *103*, 9355.
(70) Bianco, R.; Hynes, J. T. *Int. J. Quantum Chem.* **1999**, *75*, 683.
(71) Bianco, R.; Hynes, J. T. *J. Phys. Chem. A* **1999**, *103*, 3797.
(72) Xu, S. C.; Guo, R.; Wong, S. L. *Chem. Phys. Lett.* **1999**, *313*, 617.
(73) McNamara, J. P.; Tresadern, G.; Hillier, I. H. *J. Phys. Chem. A* **2000**, *104*, 4030.
(74) McNamara, J. P.; Hillier, I. H. *Phys. Chem. Chem. Phys.* **2000**, *2*, 2503.
(75) George, S. M.; Livingston, F. E. *Surf. Rev. Lett.* **1997**, *4*, 771.
(76) Frisch, M. J.; Trucks, G. W.; Schlegel, H. B.; Gill, P. M. W.; Johnson, B. G.; Robb, M. A.; Cheeseman, J. R.; Keith, T. A.; Petersson, G. A.; Montgomery, J. A.; Raghavachari, K.; Al-Laham, M. A.; Zakrzewski, V. G.; Ortiz, J. V.; Foresman, J. B.; Cioslowski, J.; Stefanov, B. B.; Nanayakkara, A.; Challacombe, M.; Peng, C. Y.; Ayala, P. Y.; Chen, W.; Wong, M. W.; Andres, J. L.; Replogle, E. S.; Gomperts, R.; Martin, R. L.; Fox, D. J.; Binkley, J. S.; Defrees, D. J.; Baker, J.; Stewart, J. P.; Head-Gordon, M.; Gonzalez, G.; Pople, J. A. *GAUSSIAN94*, revision E.1; Gaussian, Inc.: Pittsburgh, PA, 1995.
(77) Frisch, M. J.; Trucks, G. W.; Schlegel, H. B.; Scuseria, G. E.; Robb, M. A.; Cheeseman, J. R.; Zakrzewski, V. G.; Montgomery, J. A.; Stratmann, R. E.; Burant, J. C.; Dapprich, S.; Millam, J. M.; Daniels, A. D.; Kudin, K. N.; Strain, M. C.; Farkas, O.; Tomasi, J.; Barone, V.; Cossi, M.; Cammi, R.; Mennucci, K.; Pomelli, C.; Adamo, C.; Clifford, S.; Ochterski, J.; Petersson, G. A.; Ayala, P. Y.; Cui, Q.; Morokuma, K.; Malick, D. K.; Rabuck, A. D.; Raghavachari, K.; Foresman, J. B.; Cioslowski, J.; Ortiz, J. V.; Stefanov, B. B.; Liu, G.; Liashenko, A.; Piskorz, P.; Komaromi, I.; Gomperts, R.; Martin, R. L.; Fox, D. J.; Keith, T.; Al-Laham, M. A.; Peng, C. Y.; Nanayakkara, A.; Gonzalez, C.; Challacombe, M.; Gill, P. M. W.; Johnson, B. G.; Chen, W.; Wong, M. W.; Andres, J. L.; Head-Gordon, M.; Replogle, E. S.; Pople, J. A. *GAUSSIAN98*, revision A.7; Gaussian, Inc.: Pittsburgh, PA, 1998.
(78) Lee, C.; Yang, W.; Parr, R. G. *Phys. Rev. B* **1988**, *37*, 785.
(79) Miehlich, B.; Savin, A.; Stoll, H.; Preuss, H. *Chem. Phys. Lett.* **1989**, *157*, 200.
(80) Becke, A. D. *J. Chem. Phys.* **1993**, *98*, 5648.
(81) Møller, C.; Plesset, M. S. *Phys. Rev.* **1934**, *46*, 618.
(82) Casper, B.; Lambotte, P.; Minkwitz, R.; Oberhammer, H. *J. Phys. Chem.* **1993**, *97*, 9992.
(83) Ehara, M.; Ohtsuka, Y.; Nakatsuji, H. *Chem. Phys. Lett.* **1998**, *226*, 113.
(84) Rayez, M. T.; Destriau, M. *Chem. Phys. Lett.* **1993**, *206*, 278.
(85) Hanson, D. R.; *J. Phys. Chem.* **1995**, *99*, 13059.
(86) Bianco, R.; Thompson, W. H.; Morita, A.; Hynes, J. T. *J. Phys. Chem. A* **2001**, *105*, 3132.
(87) Tabazadeh, A.; Turco, R. P. *J. Geophys. Res.* **1993**, *98*, 12727.
(88) Bell, R. P.; Gelles, E. *J. Chem. Soc.* **1951**, 2734.
(89) Eigen, M.; Kustin, K. *J. Am. Chem. Soc.* **1962**, *84*, 1355.
(90) Francisco, J. S.; Sander, S. P. *J. Chem. Phys.* **1995**, *102*, 9615.
(91) Manuel, M.; Mó, O.; Yáñez, M. *J. Phys. Chem. A* **1997**, *101*, 1722.